2010

PREDICTING RUNOFF AND SEDIMENT YIELD USING SWAT MODEL FOR IJA GALMA WAQO SPATE IRRIGATION PROJECT

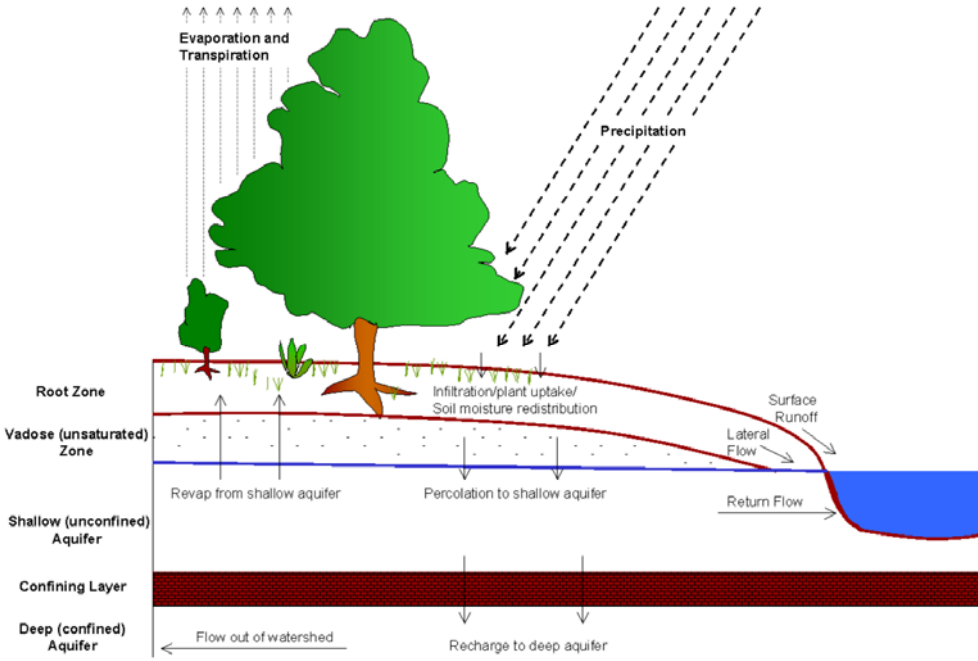

EYOB YEHAYIS

HARAMAYA UNIVERSITY

1/21/2010

PREDICTING RUNOFF AND SEDIMENT YIELD USING SWAT MODEL FOR IJA GALMA WAQO SPATE IRRIGATION PROJECT

A Thesis Submitted to Institute of Technology, School of Natural Resource and Environmental Engineering
HARAMAYA UNIVERSITY

In Partial Fulfillment of the Requirement for the Degree of
MASTER OF SCIENCE IN IRRIGATION ENGINEERING

By
EYOB YEHAYIS

January 2010
Haramaya University

School of Graduate Studies
Haramaya University

As Thesis research advisor, I herby certify that I have read and evaluated this Thesis prepared, under my guidance, by **Eyob Yeheyies,** entitled **Predicting Runoff and Sediment Yield Using SWAT Model for Ija Galma Waqo Spate Irrigation Project.**

Dr. Tena Alamirew		
Major Advisor	Signature	Date

As member of the *Board of Examiners* of the MSc Thesis Open Defense Examination, we certify that we have read, evaluated the thesis prepared by **Eyob Yeheyies** and examined the candidate. We recommended that the thesis be accepted as fulfilling the Thesis requirement for the degree of *Master of Science* in Irrigation Engineering.

Dr. Shoeb Quraishi		21.01.12
Chairperson	Signature	Date
Dr. Desalegn Chemeda		21/01/10
Internal Examiner	Signature	Date
Dr. Fantaw Abegaz		21/01/10
External Examiner	Signature	Date

DEDICATION

I dedicate this thesis manuscript to my mother Yeshi Fekadu, my wife Misrak Fetene and our children, Yisakor and Heaven Eyob, and also for my brothers and sisters for their affection, love and their generous moral support during my studies.

STATEMENT OF THE AUTHOR

First, I declare that this thesis is my work and that all sources of materials used for this thesis have been duly acknowledged. This Thesis has been submitted in partial fulfillment of the requirements for an advanced M.Sc. degree at the Haramaya University and deposited at the University Library to be made available to borrowers under rules of the Library.

Brief quotations from this Thesis are allowable without special permission provided that accurate acknowledgement of sources is made. Requests for permission for extended quotations from or reproduction of this manuscript in whole or in part may be granted by the head of the School of Natural Resources and Environmental Engineering or the dean of the School of Graduate Studies when in his or her judgment the proposed use of the material is in the interests of scholarship. In all other instances, however, permission must be obtained from the author.

Eyob Yehayis
Haramaya University, Haramaya

Signature:……

ABBREVIATIONS

Arc SWAT	Swat Integrated with ArcGIS
Alpha_Bf	Alpha base factor
Biomx	Biological mixing efficiency
Canmx	Maximum canopy storage
BMP	Best Management Practices
CDF	Cumulative Density Function
Ch_N	Main canal Manning's roughness coefficient
Cn2	Moisture Condition Curve Number
DEM	Digital Elevation Model
DWSM	Water Simulation Model
EPIC	Erosion-Productivity Impact Calculator
EHRS	Ethiopian Highland Reclamation Study
Epco	Plant uptake composition factor
Esco	Soil Evaporation Compensation Factor
ET	Evapotranspiration
EU	European Union
FAO	Food and Agriculture Organization
GIS	Geographic Information System
GLEAMS	Groundwater Loading Effects On Agricultural Management Systems
GW_Delay	Groundwater Delay Time
GW_Revap	Groundwater Revap Coefficient
GWQMN	Threshold Water Depth in the Shallow Aquifer for Flow
HRU	Hydraulic Response Unit
HSPF	Hydrological Simulation Programme FORTRAN
HUMUS	Hydrologic Unit Model for the United States
LH-OAT	Latine Hypercube and One-At-a-Time
MIKE-SHE	System Hydrologique European
MUSLE	Modified Universal Soil Loss Equation
MoWR	Ministry of Water Resource
NASA	National Aeronautics and Space Administration
NMSA	National Metrology Service Agency
NSE	Nash-Sutcliffe Efficiency
ROTO	Routing Outputs to Outlet
SCRP	Soil Conservation Research Project
Sol_Awc	Soil available water content
Sol_K	Soil saturated Hydraulic conductivity
SWRRB	Simulator for Water Resources in Rural Basins
STATSGO	State Soils Geographic Database
SRTM	Shuttle Radar Topographic Mission
SWAT	Soil Water Assessment Tool
SWIM	Soil and Water Integrated Model
SUSAT	Sub Watershed Spatial Analysis Tool

BIOGRAPHICAL SKETCH

The author was born in Gursum (Fugnan Bira), East Harargie zone, Ethiopia in August 29, 1968. He attended elementary and junior secondary school from 1976-1982 at Babile and Gursum, and secondary school from 1983-1987 at Gursum high School. After the completion of his secondary school education in 1987, he joined the then Alemaya University of Agriculture in 1988 for his undergraduate studies and graduated with B.Sc. degree in Agricultural Engineering in 1994.

Soon after graduation, the author was employed by Oromia Natural Resource Bureau in 1995. Since then he was working as an expert, site engineer in the design and construction of a number of irrigation projects, and section and department head of Oromia Irrigation Development Authority Eastern Branch Office.

In 2008, he joined the Graduate School of the Haramaya University to pursue his M.Sc studies in the field of Soil and Water Engineering (Irrigation Engineering).

ACKNOWLEDGEMENT

First of all, I would like to thank the almighty God for giving me the life, audacity and wisdom.

I am very grateful to Oromia Water Resource Bureau for allowing me to take part in the Graduate Study Program of irrigation engineering and also my beautiful wife and friends who made my dream came true with their advice and support.

I would like to express my sincere gratitude to my supervisor, Dr Tena Alamirew for giving me valuable guidance and support throughout my research. I am also grateful to my friends, Mr. Yohanis Galeta, Teshome Seyoum, Wondu Alemayehu and Yared Mengesha who gave me the data and helpful documents and material.

I would also like to thank the Ethiopian Ministry of Water Resources, National Meteorological Services Agency and Oromia Region Water Resources, for providing me important priceless data.

Thanks to God, I have lots of exciting Ministries and friends whom I met in my walk of life. Of which Love World Christian Network and Synagogue Church of All Nations who feed my spirit with the precious word of God.

At last but not least, I would like to extend my deepest gratitude to my family, without their encouragement and care this would not have happened.

TABLE OF CONTENTS

Cont'd…

TABLE OF CONTENT (*Continued*)

LIST OF TABLES

Table **Page**

LIST OF FIGURES

Figure **Page**

LIST OF TABLES IN THE APPENDIX

Appendix Table **Page**

LIST OF FIGURES IN THE APPENDIX

Appendix Figure **Page**

"PREDICTING RUNOFF AND SEDIMENT YIELD USING SWAT MODEL FOR IJA GALMA WAQO SPATE IRRIGATION PROJECT"

ABSTRACT:

Knowledge of the internal renewable water resources of a country is strategic information which is needed for long-term planning of a nation's water and food security, among many other needs. New modeling tools allow this quantification with high spatial and temporal resolution. In this study, Soil and Water Assessment Tool (SWAT) was used to calibrate and validate a hydrologic component on Erer river discharges at gauging station and predict the water and sediment yield of Ija Galma Waqo spate irrigation. Sensitivity analysis, model calibration and validation were also performed to assess the model performance. Ten highly sensitive parameters were identified of which base flow alpha factor was the most sensitive one. The coefficient of determination (R^2) and Nash-Sutcliffe (E_{NS}) was used to evaluate model calibration and validation. The results found were satisfactory for the gauging station (R^2 = 0.65 and. E_{NS} = 0.56 for calibration and R^2 = 0.73 and. E_{NS} = 0.5 for validation period).The water and sediment yield of Ija Galma Waqo spate irrigation project was quantified and also the most sediment yielding part of the basin was identified. The result of simulation after calibration with the seasonal and annual time steps for water yield, for the Annual, Intermediate, Wet and Dry seasons were 184.2, 64.9, 67.2, and 52.1 ha-m respectively and the corresponding coefficient of variation was found to be 0.97, 1.17, 1.43, and 1.89 and also the 70 % dependable water yield were 87.50, 24.80, 21.10 and 4.40 ha-m., respectively. The predicted sediment yield for the Annual, Intermediate, Wet, and Dry season were 2.48, 1.01, 0.73 and 0.73 tons/ ha with the respective coefficient of variation 2.7, 1, 1.07, and 2.07. Among the contributing subbasins, the one which substantially contributes was identified (subbasin 6). In conclusion, the SWAT model could be effectively used to predict runoff and sediment yield in order to effectively design spate irrigation system and water related development in absence of gauged information.

1. INTRODUCTION

Ethiopia experiences persistent land, water and environmental degradation due to localized and global climatic anomalies. These leave the country to recurrent crop failures and severe food shortages. Low soil fertility coupled with temporal imbalance in the distribution of rainfall and the substantial non- availability of the required water at the required period are the principal contributing factors to the low and declining agricultural productivity. Hence, proper utilization of the available soil and water resources and development of irrigation is essential to Ethiopia's agricultural development and to achieve food security.

The poor land use practices, improper management systems and lack of appropriate soil conservation measures have played a major role for causing land degradation problems in the country. Because of the rugged terrain, the rates of soil erosion and land degradation in Ethiopia are high. The soil depth of more than 34 % of the land area is already less than 35 cm (Zemenfes, 1995; SCRP, 1996). Hurni (1989) indicated that Ethiopia loses about 1.3 billion metric tons of fertile soil every year and the degradation of land through soil erosion is increasing at a high rate. According to Kruger *et al*, (1996) 4% of the highlands are so seriously eroded that they will not be economically productive again in a predictable future. The Soil Conservation Research Project (SCRP, 1996) has estimated an annual soil loss of about 1.5 billion tons from the highland. According to the Ethiopian Highlands Reclamation Study (EHRS, 1984) soil erosion is estimated to cost the country 1.9 billion US$ between 1985 and 2010. These call for immediate measures to save the physical quality of soil and water resources of the country.

A river is not only conveying water, but has much other function. One of these functions is transporting of erosion products (boulders gravel, sand, silt and clay) from its catchment in downstream direction. If the transport capacity of the river is affected by diversion of water from the river or by storing water in the reservoir, deposition of sediment may occur. If not properly taken care of, harmful sedimentation and erosion may occur. Many reservoirs are suffering from excessive sedimentation often due to the fact that either the upstream sediment supply was never considered or that the seriousness of this process is underestimated, because of the lack of sufficient data availability. Also a change in sediment yield is due to changed land use in the

upstream catchment that can cause detrimental sedimentation (for instance Haramaya Lake is one such example).

Many main canals of irrigation projects suffer from excessive sedimentation which is entering via the headwork. Often this is due to the fact that the sediment transport in the river was not properly assessed and appears to be much larger than anticipated. Another reason is that morphological changes have taken place after construction of the intake structure, which jeopardized the measure taken to exclude sediment when withdrawing water. Among these victims, Bililo Spate irrigation project is one of them.

A systematic assessment of water resources availability with high spatial and temporal resolution is essential in Ethiopia for strategic decision-making on water resource related development projects. Although empirical formulas are adopted, which simply simulates rainfall runoff relationship which is developed in other similar agro climatic zone. There is a great uncertainty on the estimations because it does not consider complex interaction that takes place in the watershed.

Therefore, a comprehensive understanding of hydrological process in the watershed is the pre-requisite for successful water management and environmental restoration. Due to the spatial and temporal heterogeneity in soil properties, vegetation and land use practices, a hydrologic cycle is a complex system. As a result mathematical model and geospatial analysis tool are required for studying hydrological process and hydrological responses to land use and climatic changes. Hence to analyze the yield of Ija Galma Waqo stream watershed with respect to quantity and quality of runoff is essential for the proper and sustainable utilization of Ija Galma Waqo Spate Irrigation Project. Although most spate irrigation projects were characterized by high sediment transport, a proper investigation of the sediment and runoff yield of the catchment is essential for management of sedimentation and utilization of water resource. If these are not investigated the life of the project is shortened by sedimentation on the farm land and canal system, as well as it makes difficult to design the appropriate and economical structures. Moreover, it makes difficult to select the appropriate crop type scheduling with respect to available runoff. In this project, stream flow rate with respect to day, month and year with its respective sediment concentration

is not known. This is due to the absence of river gauge records and lack of adopting or use of different hydrologic model relevant for the required objectives.

This work is intended to provide a basis for future scenario analysis of water resource management of this project and also to evaluate the SWAT model capability to predict the runoff yield of the project.

Against this backdrop, the main objectives of this study were:

1. To estimate the catchment runoff and sediment yield using SWAT model at the headwork site on a monthly and yearly time-step, and
2. To identify the most problematic sub basin with respect to sedimentation.

2. LITRATURE REVIEW

2.1. Impact of Land Use on Water Resource

2.1.1. Land use impact on hydrologic regime

With regard to the hydrologic regime, impacts on surface and ground water resources can be distinguished. Impacts of land use practices on surface water can be divided into (i) impacts on the overall water availability or the mean annual runoff, and (ii) impacts on the seasonal distribution of water availability. With regard to the latter, impacts on peak flows and impacts on dry season flows are of importance. With regard to groundwater, the effect of the land use on groundwater recharge has to be examined.

2.1.1.1. Mean surface runoff

The impact of land use on the mean runoff is a function of many variables, the most important being the water regime of the plant cover in terms of evapotranspiration (ET), the ability of the soil to hold water, and the ability of the plant cover to intercept moisture.

A change of land cover from lower to higher ET will lead to a decrease in annual stream flow. From a review of 94 catchment experiments, Bosch and Hewlett (1982) concluded that the establishment of forest cover on sparsely vegetated land decreases water yield. Coniferous forest, deciduous hardwood, brush and grass cover have (in that order) a decreasing influence on water yield of the source areas in which the covers are manipulated. Conversely, a change from higher-ET plants to lower-ET plants will increase the mean surface runoff: reduction in forest cover increases water yield (Bosch and Hewlett, 1982; Calder, 1998). The impact, however, depends very much on the management practices and the alternative land uses. Careful, selective harvesting of timber has no or little effect on stream flow. Stream flow after maturation of the new plant cover may be higher, the same or lower than original value, depending on vegetation (Bruijnzeel, 1990).

An exception to this rule are cloud forests, which can intercept more moisture (fog drip) than consumption by ET and very old forests, which, depending on the species, may consume less

water than the vegetation that establishes itself after clear-cutting (Calder, 1998). Stream flow gains decline over time with establishment of new plant cover, but time scales can vary greatly. In humid warm areas, the effect of clear-cutting is shorter lived than in less humid areas, due to rapid re-growth of vegetation (Falkenmark and Chapman, 1989). Increasing water yield from changing plant cover does not necessarily increase water availability downstream. Stream flow might decrease because of other factors, e.g. water consumption by riparian vegetation or through transmission losses (Brooks *et al.,* 1991).

2.1.1.2. Peak flow/floods

Peak flows can increase as a result of a change in land use if the infiltration capacity of the soil is reduced, for example through soil compaction or erosion, or if drainage capacity is increased. Peak flow may increase after trees are cut down (Bruijnzeel, 1990). Relative increases in storm flow after tree removal is smallest for large events and largest for small events. As the amount of precipitation increases, influence on storm flow of soil and plant cover diminishes (Bruijnzeel, 1990).

An increase of peak flows may also result from the building of roads and infrastructure. Studies in the north-western USA have shown that the construction of forest roads can intensify peak runoff from forested areas significantly (Bowling and Lettenmaier, 1997; La Marche and Lettenmaier, 1998). Consolidation of smaller plots to large fields can lead to higher runoff rates, due to drainage systems and asphalt access roads (Falkenmark and Chapin, 1989). Conversely, peak flows may decrease as a result of an increased soil infiltration capacity.

In larger basins, effects of land use practices on peak flow are offset due to time lag between different tributaries, different land use and variations in rainfall (Bruijnzeel, 1990). In larger watersheds, this de-synchronization effect can lead to a reduction in peak discharge, although overall storm flow increases due to land use changes in individual sub watersheds (Brooks *et al.,* 1991).

2.1.1.3. Base flow/dry season flow

The effect of land use change on dry-season flow depends on competing processes, most notably changes in ET and infiltration capacity. The net impact is likely to be highly site specific (Calder, 1998).

In tropical areas, afforestation can lead to decreased dry-season flows due to increased evapotranspiration. In the Mae Thang watershed (Thailand), afforestation programs led to water shortages downstream, which resulted in a seasonal closure of a water treatment plant and lower availability for irrigation (Chomitz and Kumari, 1996). Similarly, in the Fiji Islands, large-scale pine afforestation (60 000 ha) in watersheds previously covered by grassland led to reductions in dry-season flow of 50-60 percent, putting the operation of a hydro-electric plant and drinking water supply at risk (FAO, 1987).

Most experimental evidence in rainfall-dominated regimes suggests that forest removal (or change from high-water-use plants to low-water-use plants) increases dry season flows (Brooks *et al.,* 1991). In contrast, dry-season flows from deforested land may decrease if the soil infiltration capacity is reduced, e.g. through use of heavy machinery (Bruijnzeel, 1990). Low flow resulting from extended dry periods or droughts may not be substantially altered by changes in vegetative cover (Brooks *et al.,* 1991).

2.1.1.4. Groundwater recharge

The groundwater recharge may be increased or decreased as a result of changing land use practices. The major driving forces are the ET of the vegetative cover and the infiltration capacity of the soil. Groundwater recharge is often linked with dry-season flows, as groundwater contributes much of the river discharge during the dry season. The water table may rise as a result of decreased evapotranspiration, e.g. following logging or conversion of forest to grassland for grazing. Recharge may also increase due to an increased infiltration rate, e.g. through afforestation of degraded areas (Tejwani, 1993).

In contrast, the water table may fall as a result of decreased soil infiltration, e.g. through non-conservation farming techniques and compaction (Tejwani, 1993). And also, heavy grazing may lead to reduced infiltration and groundwater recharge (Chomitz and Kumari, 1996). If the infiltration capacity is substantially reduced, this can lead to water shortages in dry seasons, even in regions where water is usually abundant, like in the case of shifting cultivation in Cherapunji province, India (FAO, 1999). Likewise, groundwater recharge can be reduced as a result of planting of deep rooting tree species, e.g. eucalyptus (Calder, 1998).

2.1.2. Impact of land use on erosion and sediment load

Forests are checkers of soil erosion. Protection is largely because of under storey vegetation and litter, and the stabilizing effect of the root network. On steep slopes, the net stabilizing effect of trees is usually positive. Vegetation cover can prevent the occurrence of shallow landslides (Bruijnzeel, 1990). However, large landslides on steep terrain are not influenced appreciably by vegetation cover. These large slides may contribute the bulk of the sediment, as for example in the middle hills of the Himalayas (Bruijnzeel and Bremmer, 1989).

Afforestation does not necessarily decrease soil erosion. Splash erosion may increase substantially when litter is cleared from the forest floor (Bruijnzeel, 1990). The spectrum for the size of the drops that are formed by the canopy varies widely among different species, resulting in large differences in the potential of splash erosion (Calder, 1998).

Deforestation may increase erosion. In Malaysia, streams from logged areas carry 8-17 times more sediment load than before logging (Falkenmark and Chapman, 1989). The actual soil loss, however, depends largely on the use to which the land is put after the trees have been cleared. Surface erosion from well-kept grassland, moderately grazed forests and soil-conserving agriculture are low to moderate (Bruijnzeel, 1990). Road construction may be a major cause for erosion during timber harvesting operations. In the USA, forest roads are estimated to account for 90 percent of the erosion caused by logging activities (Brooks *et al.,* 1991; Bruijnzeel, 1990).

Effects of erosion control measures on sediment yield will be most readily felt on-site. There is an inverse relation between basin size and sediment delivery ratio. In basins of several hundred

km^2 improvements may only be noticeable after a considerable time lag (Decades), due to storage effects (Bruijnzeel, 1990). Downstream sediment yields cannot always be ascribed to the changing of upstream land use practices. Human impacts on sediment yield may be substantial in regions with stable geological conditions and low natural erosion rates. In regions with high rainfall rates, steep terrain, and high natural erosion rates, however, the impact of land use may be negligible. In the Phewa Tal watershed in Nepal, for example, only six percent of the total sediment yield has been calculated to stem from surface erosion (Bruijnzeel, 1990). Sediment can act both as a physical and a chemical pollutant. Physical pollution characteristics of sediment include turbidity (limited penetration of sunlight) and sedimentation (loss of downstream reservoir capacity, destruction of coral reefs, and loss of spawning grounds for certain fish).

2.2. Scale Consideration

The above review of land use impacts on water resources does not take into account spatial and temporal distribution aspects. Scale considerations, however, are of fundamental importance when assessing these impacts as they indicate whether a land use upstream may affect a water use downstream.

2.2.1. Spatial scale

With regard to the spatial scale, i.e. the size of river basin, the land use impact can become less important because of offset effects, such as de-synchronization (e.g. in the case of floods), storage capacity of the river bed (sedimentation) or the self-cleaning capacity of the river (organic pollution). At the same time, the impact can become more important with increasing scale due to accumulative effects, e.g. in the case of salinity.

Land use induced changes of the hydrologic regime and sediment load decrease with the size of the river basin. The effects will be most readily felt in smaller watersheds of up to several hundred km^2. One well-documented case is the Ganges-Brahmaputra-Meghan basin. Studies show that in small-scale catchments (<50 km^2) in the basin, erosion and stream flow may be strongly influenced by changing land use patterns (Ives and Messerli, 1989). However, the lowland flooding in Bangladesh is not related to the increased peak flow and erosion resulting

from deforestation in the Himalayan uplands in Nepal. The main driving forces behind the flood events in the plains are naturally occurring rainfall events in the lowlands, which may be augmented by human interventions in the floodplains, such as road and river embankments (Ives and Messerli, 1989; Hofer, 1998). Similarly, the bulk of the sediment load in the Ganges-Brahmaputra river system does not stem from human-induced erosion, but rather from large landslides not influenced by human activity (Bruijnzeel and Bremmer, 1989).

With regard to water quality impacts, the picture is much less clear. Observations show that some land use impacts on water quality, like salinity or pesticide load, can also have downstream effects in medium to large watersheds, like the Murray-Darling basin (Australia) and the Colorado basin (USA/Mexico). Other downstream impacts, like organic matter and pathogens are relevant only at smaller scales.

2.2.2. Temporal scale

Temporal scale is another important aspect of land use impacts, as it determines the perception of the impact as well as the economic cost associated with it. Two aspects are important with regard to temporal scale of land use impacts. First, the time it takes for a land use to have an impact on downstream uses, and, second, in the case of negative impacts, the time it takes for remedial measures to take effect, if the impact is reversible.

The temporal scales of land use impacts vary widely. Depending on the impact, they may range from less than one year, as in the case of bacterial contamination, to hundreds of years, as in the case of salinity. Similarly, time scales of recovery from adverse impacts are very diverse, depending on the impact. However, in most cases, the time it takes to restore an aquatic system after an adverse impact is much longer than the time it takes for an impact to appear (Peters and Meybeck, 2000).

Generally, with regard to land use impacts on hydrologic regimes and sediment transport, there is an inverse relationship between the spatial scale in which the impacts can be observed and the scale in which the redistribution of benefits might be important. These impacts can be most readily felt in small spatial scales. At the same time, the number of water users who might

benefit or suffer from this land use change, increases with the size of the watershed. Due to the decreasing magnitude of impact, the respective costs and benefits will be small. Impacts of land use practices on water quality, like salinity, pesticide pollution and eutrophication due to nutrient influx, however, may be relevant in medium to large-scale river basins as well. These impacts may affect many downstream uses, including providers of drinking water, industries, fisheries and other agricultural uses.

2.3. SWAT Development and Interface

SWAT (Arnold *et al.,* 1998) is a semi-distributed, time continuous watershed simulator operating on a daily time step. It is developed for assessing the impact of management and climate on water supplies, sediment, and agricultural chemical yields in watersheds and larger river basins. The model is semi-physically based, and allows simulation of a high level of spatial detail by dividing the watershed into a large number of sub-watersheds. The major components of SWAT include hydrology, weather, erosion, plant growth, nutrients, pesticides, land management, and stream routing. The program is provided with an interface in Arc GIS (Arc SWAT 2005, Winchell *et al.,* 2008) for the definition of watershed hydrologic features and storage, as well as the organization and manipulation of the related spatial and tabular data.

2.3.1. Theoretical description of SWAT

The large scale spatial heterogeneity of the study area is represented by dividing the watershed into subbasins. Each subbasin is further discretised into a series of hydrologic response units (HRUs), which are unique soil-land use combinations. Soil water content, surface runoff, nutrient cycles, sediment yield, crop growth and management practices are simulated for each HRU and then aggregated for the subbasin by a weighted average.

Physical characteristics, such as slope, reach dimensions, and climatic data are considered for each subbasin. For climate, SWAT uses the data from the station nearest to the centric of each subbasin. Calculated flow, sediment yield, and nutrient loading obtained for each subbasins are then routed through the river system. Channel routing is simulated using the variable storage or Muskingum method.

The water in each HRU in SWAT is stored in four storage volumes: snow, soil profile (0–2 m), shallow aquifer (typically 2–20 m), and deep aquifer. Surface runoff from daily rainfall is estimated using a modified SCS curve number method, which estimates the amount of runoff based on local land use, soil type, and antecedent moisture condition. Peak runoff predictions are based on a modification of the Rational Formula (Chow *et al.,* 1988). The watershed concentration time is estimated using Manning's formula, considering both overland and channel flow.

The soil profile is subdivided into multiple layers that support soil water processes including infiltration, evaporation, plant uptake, lateral flow, and percolation to lower layers. The soil percolation component of SWAT uses a water storage capacity technique to predict flow through each soil layer in the root zone. Downward flow occurs when field capacity of a soil layer is exceeded and the layer below is not saturated. Percolation from the bottom of the soil profile recharges the shallow aquifer.

Daily average soil temperature is simulated as a function of the maximum and minimum air temperature. If the temperature in a particular layer reaches less than or equal to 0^{o}C, no percolation is allowed from that layer. Lateral sub-surface flow in the soil profile is calculated simultaneously with percolation. Groundwater flow contribution to total stream flow is simulated by routing a shallow aquifer storage component to the stream (Arnold and Allen, 1996).

The model computes evaporation from soils and plants separately. Potential evapotranspiration can be modeled with the Penman–Monteith (Monteith, 1965), Priestley–Taylor (Priestley and Taylor, 1972), or Hargreaves methods (Hargreaves and Samani, 1985), depending on data availability. Potential soil water evaporation is estimated as a function of potential ET and leaf area index (area of plant leaves relative to the soil surface area). Actual soil evaporation is estimated by using exponential functions of soil depth and water content. Plant water evaporation is simulated as a linear function of potential ET, leaf area index, and root depth, and can be limited by soil water content. More detailed descriptions of the model can be found in Arnold *et al.* (1998).

Sediment yield in SWAT is estimated with the modified soil loss equation (MUSLE) developed by Wischmeier and Smith (1978). The sediment routing model consists of two components operating simultaneously: deposition and degradation. The deposition in the channel and floodplain from the sub-watershed to the watershed outlet is based on the sediment particle settling velocity. The settling velocity is determined using Stoke's law (Chow *et al.,* 1988) and is calculated as a function of particle diameter squared. The depth of fall through a reach is the product of settling velocity and the reach travel time. The delivery ratio is estimated for each particle size as a linear function of fall velocity, travel time, and flow depth. Degradation in the channel is based on Bagnold's stream power concept (Bagnold, 1977; Williams, 1980) generally some of the components related to the study are below:

2.3.2. Hydrological component of SWAT

Simulation of hydrology of a watershed is done in two separate components. One is the land phase of the hydrologic cycle that controls the water movement in the land and determines the water, sediment, nutrient and pesticide amount that will be loaded into the main stream. Hydrological components simulated in land phase of the Hydrological cycle are canopy storage, infiltration, redistribution, and evapotranspiration, lateral subsurface flow, surface runoff, ponds and tributary channels return flow. The second component is routing phase of the hydrological cycle in which the water is routed in the channels network of the watershed, carrying the sediment, nutrients and pesticides to the outlet. In the land phase of the hydrologic cycle, SWAT simulates the hydrological cycle based on the water balance equation.

$$SWt = SW_0 + \sum (R_{day} - Q_{surf} - E_a - W_{seep} - Q_{gw}) \quad 1$$

Where SWt is the final soil water content (mm), SW_0 is the initial soil water content for day i (mm), t is the days (days), R_{day} is the day precipitation (mm), Q_{surf} is the surface runoff (mm), E_a is the evapotranspiration (mm), W_{seep} is the seepage from the bottom soil layer (mm) and Q_{gw} is the groundwater flow on day i (mm).

Brief description of some of the key model components are provided in this study. More detailed descriptions of the different model components are listed in Arnold *et al.,* (1998), Neitsch *et al.,*

(2005).Surface runoff occurs whenever the rate of precipitation exceeds the rate of infiltration. SWAT offers two methods for estimating surface runoff: the SCS curve number procedure (USDA-SCS, 1972) and the Green & Ampt infiltration method (Green and Ampt, 1911). Using daily or sub daily rainfall, SWAT simulates surface runoff volumes and peak runoff rates for each HRU. The SCS curve number equation is (SCS, 1972):

$$Q_{surf} = \frac{\left(R_{day} - 0.2S\right)^2}{\left(R_{day} + 0.8S\right)} \qquad 2$$

In which, Q_{surf} is the accumulated runoff or rainfall excess (mm), R_{day} is the rainfall depth for the day (mm), S is the retention parameter (mm). The retention parameter is defined by equation 3.

$$S = 25.4\left(\frac{1000}{CN} - 10\right) \qquad 3$$

Swat2005 version includes two methods for calculating the retention parameter; the first one is retention parameter varies with soil profile water content and the second method is the retention parameter varies with accumulated plant evapotranspiration. The soil moisture method (equation 4), over estimate runoff in shallow soils. But calculating daily CN as a function of plant evapotranspiration, the value is less dependent on soil storage and more dependent on antecedent climate.

$$S = S_{\max} \cdot \left(1 - \frac{SW}{\left[SW + \exp\left(w_1 - w_2 \cdot SW\right)\right]}\right) \qquad 4$$

Where S is the retention parameter for a given day (mm), S_{max} is the maximum value the retention parameter can achieve on any given day (mm), SW is the soil water content of the entire profile excluding the amount of water held in the profile at wilting point (mm), and w_1 and w_2 are shape coefficients. The maximum retention parameter value, S_{max}, is calculated by solving equation 5 using CN_1.

$$\text{Smax} = 25.4\left(\frac{1000}{CN_1} - 10\right) \quad (5)$$

When the retention parameter varies with plant evapotranspiration, the following equation is used to update the retention parameter at the end of every day:

$$S = S_{prev} + E_o * \exp\left(\frac{-cncoef - S_{prev}}{S_{\max}}\right) - R_{day} - Q_{surf} \quad (6)$$

Where S is the retention parameter for a given day (mm), S_{prev} is the retention parameter for the previous day (mm), E_o is the potential evapotranspiration for the day (mm d^{-1}), *cncoef* is the weighting coefficient used to calculate the retention coefficient for daily curve number calculations dependent on plant evapotranspiration, S_{max} is the maximum value the retention parameter can achieve on any given day (mm), R_{day} is the rainfall depth for the day (mm), and Q_{surf} is the surface runoff (mm). The initial value of the retention parameter is defined as $S = 0.9xS_{\max}$.

The SCS curve number is a function of the soil permeability, land use and antecedent soil water condition. SCS defines three antecedent moisture conditions: I—dry (wilting point), II—average moisture, and III—wet (field capacity). The moisture condition I curve number is the lowest value the daily curve number can assume in dry conditions. The curve numbers for moisture conditions I and III are calculated with equations 7 and 8, respectively.

$$CN_1 = CN_2 - \frac{20 \cdot (100 - CN_2)}{(100 - CN_2 + \exp[2.533 - 0.0636 \cdot (100 - CN_2)])} \quad (7)$$

$$CN_3 = CN_2 \cdot \exp[0.00673 \cdot (100 - CN_2)] \quad (8)$$

Where CN_1 is the moisture condition I curve number, CN_2 is the moisture condition II curve number, and CN_3 is the moisture condition III curve number.

Typical curve numbers for moisture condition II are listed in various tables (Neitsch *et al.*, 2005), for various land covers and soil types. These values are appropriate for a slope of 5%. Williams (1995) developed an equation to adjust the curve number to a different slope:

$$CN_{2s} = \frac{(CN_3 - CN_2)}{3} \cdot [1 - 2 \cdot \exp(-13.86 \cdot slp)] + CN_2 \qquad 9$$

Where CN_{2s} is the moisture condition II curve number adjusted for slope, CN_3 is the moisture condition III curve number for the default 5% slope, CN_2 is the moisture condition II curve number for the default 5% slope, and *slp* is the average percent slope of the subbasin.

SWAT calculates the peak runoff rate with a modified rational method. Numerous methods have been developed to estimate Potential evapotranspiration (PET). Three of these methods have been incorporated into SWAT: the Penman-Monteith method (Monteith, 1965; Allen, 1986; Allen *et al.,* 1989), the Priestley-Taylor method (Priestley and Taylor, 1972) and the Hargreaves method (Hargreaves *et al.,* 1985).

The simulation of ground water is done into two aquifers in each subbasin. That is the shallow and the deep aquifer. The shallow aquifer is an unconfined aquifer that contributes to flow in the main channel or reach of the subbasin. The deep aquifer is a confined aquifer. Water that enters the deep aquifer is assumed to contribute to stream flow somewhere outside of the watershed (Arnold, 1993). In SWAT 2005 the water balance for the shallow aquifer is calculated with equation 10.

$$aq_{sh,i} = aq_{sh,i-1} + w_{rchrg,sh} - Q_{gw} - w_{revap} - w_{pump,sh} \qquad 10$$

Where $aq_{sh,i}$ is the amount of water stored in the shallow aquifer on day i (mm), $aq_{sh,i\text{-}1}$ is the amount of water stored in the shallow aquifer on day i-1 (mm), $w_{rchrg,sh}$ is the amount of recharge entering the shallow aquifer on day i (mm), Q_{gw} is the groundwater flow, or base flow, into the main channel on day i (mm), w_{revap} is the amount of water moving into the soil zone in response to water deficiencies on day i (mm), and $w_{pump,sh}$ is the amount of water removed from the

shallow aquifer by pumping on day i (mm). The steady-state response of groundwater flow to recharge is estimated by equation 11 (Hooghoudt, 1940):

$$Q_{gw} = \frac{8000 \cdot K_{sat}}{L_{gw}^{\ 2}} \cdot h_{wtbl} \qquad 11$$

Where Q_{gw} is the groundwater flow, or base flow, into the main channel on day i (mm), K_{sat} is the hydraulic conductivity of the aquifer (mm/day), L_{gw} is the distance from the ridge or subbasin divide for the groundwater system to the main channel (m), and h_{wtbl} is the water table height (m). A water table fluctuation due to non-steady-state response of groundwater flow to periodic recharge is calculated by equation 12 (Smedema and Rycroft, 1983):

$$\frac{dh_{wtbl}}{dt} = \frac{w_{rchrg,sh} - Q_{gw}}{800 \cdot \mu} \qquad 12$$

Where $\frac{dh_{wtbl}}{dt}$ is the change in water table height with time (mm/day), $w_{rchrg,sh}$ is the amount of recharge entering the shallow aquifer on day i (mm), Q_{gw} is the groundwater flow into the main channel on day i (mm), and μ is the specific yield of the shallow aquifer (m/m). Assuming that variation in groundwater flow is linearly related to the rate of change in water table height, equations 11 and 12 can be combined to obtain:

$$\frac{dQ_{gw}}{dt} = 10 \cdot \frac{K_{sat}}{\mu \cdot L_{gw}^{\ 2}} \cdot \left(w_{rchrg,sh} - Q_{gw}\right) = \alpha_{gw} \cdot \left(w_{rchrg,sh} - Q_{gw}\right) \qquad 13$$

Where Q_{gw} is the groundwater flow into the main channel on day i (mm), K_{sat} is the hydraulic conductivity of the aquifer (mm/day), μ is the specific yield of the shallow aquifer (m/m), L_{gw} is the distance from the ridge or subbasin divide for the groundwater system to the main channel (m), $w_{rchrg,sh}$ is the amount of recharge entering the shallow aquifer on day i (mm) and α_{gw} is the base flow recession constant or constant of proportionality. The base flow recession constant, α_{gw}, is a direct index of groundwater flow response to changes in recharge (Smedema and

Rycroft, 1983). Values vary from 0.1-0.3 for land with slow response to recharge to 0.9-1.0 for land with a rapid response. Although the base flow recession constant may be calculated, the best estimates are obtained by analyzing measured stream flow during periods of no recharge in the watershed.

2.3.3. Sediment component of SWAT

SWAT computes erosion caused by rainfall and runoff with the Modified Universal Soil Loss Equation (MUSLE) (Williams, 1975). The modified universal soil loss equation (Williams, 1995) is given by equation 14:

$$sed = 11.8 \cdot \left(Q_{surf} \cdot q_{peak} \cdot area_{hru}\right)^{0.56} \cdot K_{USLE} \cdot C_{USLE} \cdot P_{USLE} \cdot LS_{USLE} \cdot CFRG \qquad 14$$

Where *sed* is the sediment yield on a given day (metric tons), Q_{surf} is the surface runoff volume (mm/ha), q_{peak} is the peak runoff rate (m^3/s), $area_{hru}$ is the area of the HRU (ha), K_{USLE} is the USLE soil erodibility factor, C_{USLE} is the USLE cover and management factor, P_{USLE} is the USLE support practice factor, LS_{USLE} is the USLE topographic factor and *CFRG* is the coarse fragment factor. The detail of the USLE factor and description of the different model components can be found in Neitsch *et al.,* (2005}

In SWAT water is routed through the channels network using either the variable storage routing or Muskingum river routing method. The detail of the water routing methods are discussed in the Neitsh *et al*. (2005). The sediment routing model Arnold (1995) that simulates the sediment transport in the channel network consists of two components operating simultaneously: deposition and degradation. To determine the deposition and degradation processes the maximum concentration of sediment calculated by equation 15 in the reach is compared to the concentration of sediment in the reach at the beginning of the time step. A brief description of sediment routing component of SWAT 2005 is given below (Neitsch *et al.,* 2005).The maximum amount of sediment that can be transported from a reach segment is a function of the peak channel velocity and is calculated by equation 15.

$$conc_{sed,ch,mx} = c_{sp} \cdot v_{ch,pk}^{\ spexp} \quad 15$$

Where $conc_{sed,ch,mx}$ is the maximum concentration of sediment that can be transported by the water (ton/m^3 or kg/L), c_{sp} is a coefficient defined by the user, $v_{ch,pk}$ is the peak channel velocity (m/s), and *spexp* is an exponent defined by the user. The exponent, *spexp*, normally varies between 1.0 and 2.0 and was set at 1.5 in the original Bagnold stream power equation (Arnold, 1995).

The maximum concentration of sediment calculated with equation 15 is compared to the concentration of sediment in the reach at the beginning of the time step, $conc_{sed,ch,i}$. If $conc_{sed,ch,i} > conc_{sed,ch,mx}$, deposition is the dominant process in the reach segment and the net amount of sediment deposited is calculated by equation 16. If $conc_{sed,ch,i} < conc_{sed,ch,mx}$, degradation is the dominant process in the reach segment and the net amount of sediment re-entrained is calculated by equation 17.

$$sed_{dep} = \left(conc_{sed,ch,i} - conc_{sed,ch,mx}\right) \cdot V_{ch} \quad 16$$

$$sed_{deg} = \left(conc_{sed,ch,mx} - conc_{sed,ch,i}\right) \cdot V_{ch} \cdot K_{CH} \cdot C_{CH} \quad 17$$

Where sed_{dep} is the amount of sediment deposited in the reach segment (metric tons), $conc_{sed,\,ch,\,i}$ is the initial sediment concentration in the reach (kg/L or ton/m^3), $conc_{sed,\,ch,\,mx}$ is the maximum concentration of sediment that can be transported by the water (kg/L or ton/m^3), and V_{ch} is the volume of water in the reach segment (m^3),. sed_{deg} is the amount of sediment re entrained in the reach segment (metric tons), K_{CH} is the channel erodibility factor (cm/hr/Pa), and C_{CH} is the channel cover factor. The final amount of sediment in the reach is determined from equation 18.

$$sed_{ch} = sed_{ch,i} - sed_{dep} + sed_{deg} \quad 18$$

Where sed_{ch} is the amount of suspended sediment in the reach (metric tons), $sed_{ch,\,i}$ is the amount of suspended sediment in the reach at the beginning of the time period (metric tons), sed_{dep} is the

amount of sediment deposited in the reach segment (metric tons), and sed_{deg} is the amount of sediment re-entrained in the reach segment (metric tons).The amount of sediment transported out of the reach is calculated:

$$sed_{out} = sed_{ch} \cdot \frac{V_{out}}{V_{ch}} \qquad 19$$

Where sed_{out} is the amount of sediment transported out of the reach (metric tons), sed_{ch} is the amount of suspended sediment in the reach (metric tons), V_{out} is the volume of outflow during the time step (m^3), and V_{ch} is the volume of water in the reach segment (m^3).

2.3.4. Performance of SWAT on hydrologic studies

Several hydrologic components (surface runoff, ET, recharge, and stream flow) that are currently in SWAT have been developed and validated at smaller scales within the EPIC, GLEAMS and SWRRB models. Interactions between surface flow and subsurface flow in SWAT are based on a linked surface - subsurface flow model developed by Arnold (1993). Characteristics of this flow model include non-empirical recharge estimates, accounting of percolation, and applicability to basin-wide management assessments with a multi-component basin water budget. The flow model was validated in a 471 km^2 watershed in the Grand Prairie region near Waco, Texas. Current SWAT reach and reservoir routing routines are based on the ROTO approach (Arnold, 1995), which was developed to estimate flow and sediment yields in large basins using sub area inputs from SWRRB. Configuration of routing schemes in SWAT is based on the approach given by Arnold *et al.,* (1994).

The surface runoff, ET, and stream flow components have been refined and validated at larger scales within SWAT including a U.S. national assessment of stream flow and ET (Arnold *et al.,* 1999). Arnold and Allen (1996) used measured data from three Illinois watersheds to successfully validate surface runoff, groundwater flow, groundwater ET, ET in the soil profile, groundwater recharge and groundwater height parameters. Groundwater recharge and discharge (base flow) results from SWAT were compared to filtered estimates for the 491,700 km^2 Upper Mississippi River Basin (Arnold *et al.,* 2000). Chu and Shirmohammadi (2004) evaluated

SWAT's capability to predict surface and subsurface flow for a 33.4 km^2 watershed in Maryland. They found that SWAT was unable to simulate an extremely wet year; but with the wet year removed, the surface runoff, base flow and stream flow results were within acceptable accuracy on a monthly basis. Subsurface flow results improved with the base flow corrected.

Rosenthal *et al.,* (1995) linked GIS to SWAT and with no calibration simulated 10 years of monthly stream flow. SWAT underestimated the extreme events but had a significant coefficient of determination (R^2=0.75). Rosenthal and Hoffman (1999) successfully used SWAT and a spatial database to simulate flows, sediment, and nutrient loadings on a 9,000 km^2 watershed in central Texas to locate potential water quality monitoring sites. SWAT was successfully validated for stream flow and sediment loads for the Mill Creek watershed in Texas for 1965-68 and 1968-75 (Srinivasan *et al.,* 1998). Monthly stream flow rates were well predicted but the model overestimated stream flows in a few years during the spring/summer months (Srinivasan *et al.,* 1 998). The overestimation may be accounted for by variable rainfall during those months. SWAT also predicted soil erosion and sediment transport satisfactorily considering the model's limitations.

As part of the HUMUS (Hydrologic Unit Model for the United States) project, annual runoff and ET were validated across the entire continental U.S. (Arnold *et al.*, 1999). Monthly stream flow was also validated against measured USGS flow at several gauging stations across the U.S. (Arnold, 2000; Arnold, 1999). Bingner (1996) simulated runoff for 10 years for a watershed in northern Mississippi. The SWAT model produced reasonable results in the simulation of runoff on a daily and annual basis from multiple subbasins, with the exception of wooded subbasins.

Arnold (1999) integrated GIS with SWAT to evaluate stream flow and sediment yield data in the Texas Gulf Basin with drainage areas ranging from 10,000 to 110,000 km^2. Stream flow data from approximately 1,000 stream monitoring gages from 1960 to 1989 were used to calibrate and validate the model. Predicted average monthly stream flow data from three to six-digit were 5% higher than measured flows with standard deviations between measured and predicted be within 2%. SWAT simulated sediment yields compared reasonably well to estimated yields (from the rating curve) considering input uncertainties, sampling errors, and model assumptions.

Benaman and Shoemaker (2004) found that significant uncertainty remained with the SWAT sediment routine.

Arnold (2001) found that a simulated wetland near Dallas, Texas needed to be at or above 85% capacity for 60% of a 14-year simulation period. Conan *et al.,* (2003) found that SWAT adequately simulated the changing from wetlands to dry land for the Upper Guadiana river basin in Spain. Hernandez *et al*., (2000) utilized existing data sets (i.e., STATSGO soil database and land cover classification) for parameterize SWAT to simulate hydrologic response to land cover change for a small semi-arid watershed (1502) in southeastern, Arizona. These authors found that calibration was required to improve model efficiency for simulation of runoff depth. Mapfumo *et al.,* (2004) tested the model's ability to simulate soil-water patterns in small watersheds under three grazing intensities in Alberta, Canada. They observed that SWAT had a tendency to over predict soil-water in dry soil conditions and to under predict in wet soil conditions. Overall, the model was adequate in simulating soil-water patterns for all three watersheds with a daily time-step.

Van Liew and Garbrecht (2003) evaluated SWAT's ability to predict stream flow under varying climatic conditions for three nested sub watersheds in the Little Washita River Experimental Watershed in southwestern Oklahoma. They found that SWAT could adequately simulate runoff for dry, average, and wet climatic conditions in one sub watershed, following calibration for relatively wet years in two of the sub watersheds. Govender and Everson (2005) also found that the model performed better in drier years than in a wet year. Deliberty and Legates (2003) used SWAT to simulate soil moisture conditions in Oklahoma. Arnold (2005) validated a crack flow model for SWAT, which simulates soil moisture conditions with depth to account for flow conditions in dry weather. The crack flow model is impacted by crack potential, soil depth and soil moisture. Seasonal trends were in agreement with simulated crack volume (R^2=0.84). Measured daily surface runoff was regressed with simulated data resulting in 0.87 coefficient of determination.

2.3.5. Performance of SWAT on sediment studies

According to Pollutant loss estimations are described in roughly 50 of the peer-reviewed papers. Papers focused on validation efforts of SWAT pollutant loss routines and/or evaluation of best management practices (BMP) are discussed in this section. Initial comparisons of SWRRB-ROTO sediment output compared favorably with measured data for three watersheds in Texas (Arnold, 1995). SWAT predictions of sediment loss were further tested in nine watersheds in Texas (Srinivasan, 1998; Arnold, 1999; Santhi *et al.,* 2001; Saleh *et al.,* 2000) and single watersheds in Indiana (Arnold and Srinivasan, 1998), New York (Benaman and Shoemaker. 2005), Maryland (Chu, 2004), and India (Tripathi *et al.,* 2004). These studies varied in watershed sizes, interval and duration of measured sediment loss, validation criteria and other factors. All of the studies concluded that the SWAT sediment predictions showed general agreement with measured values, except for the New York and Maryland experiments. The analysis in the New York watershed concentrated on high-flow sediment event data, and SWAT underestimated 34 of the 35 observed sediment loads and underestimated erosion caused by snowmelt. In Maryland, monthly sediment predictions were poor but annual sediment predictions strongly agreed with annual observed sediment loss.

SWAT has been used to evaluate the environmental or economic impacts of BMPs or land use changes at a variety of scales. SWAT was used within HUMUS to conduct a national-scale analysis of the effect of management scenarios on water quantity and quality (Jayakrishnan *et al.,* 2005). SWAT results indicated that implementation of improved tillage practices can reduce sediment yields by almost 20% in Rock River in Wisconsin (Kirsch *et al.,* 2002). Chaplot *et al.,* (2004) found that adoption of no tillage, changes in nitrogen application rates, and land use changes could greatly impact nitrogen losses in the Walnut Creek Watershed in central Iowa. Further analysis of BMPs by Vache *et al*. (2002) for Walnut Creek and a second Iowa watershed indicated that large sediment reductions could be obtained, depending on BMP choice. Gitau *et al.,* (2004) determined cost-effective pollution reduction through farm level optimization of BMP placement using SWAT. SWAT studies in India include identification of critical or priority areas for soil and water management in a watershed (Tripathi *et al.,* 2003 and Kaur *et al.,* 2004), the impact of different tillage systems on nitrogen and sediment losses (Tripathi *et al.,* 2005) and the effects of replacing rice with peanut and soybean on soil loss (Tripathi *et al.,* 2005).

Generally the wide range of SWAT applications that have been described here underscores that the model is a very flexible and robust tool that can be used to simulate a variety of watershed problems. The ability of SWAT to replicate hydrologic and/or pollutant loads at a variety of spatial scales on an annual or monthly basis has been confirmed in numerous studies. However, the model performance has been inadequate in some studies, especially when comparisons of predicted output were made with time series of measured daily flow and/or pollutant loss data. Some users have addressed weaknesses in SWAT by component modifications, which support more accurate simulation of specific processes or regions. This is a trend that will likely continue. It can also be expected that additional support tools will be created in the future to facilitate various applications of SWAT. The SWAT model will continue to evolve in response to the needs of the ever-increasing worldwide user community and to provide improved simulation accuracy of key processes.

2.3.6. Sensitivity analysis

SWAT is a complex model with many parameters that makes manual calibration difficult. Hence, sensitivity analysis was performed to limit the number of optimized parameters to obtain a good fit between the simulated and measured data. Sensitivity analysis helps to determine the relative ranking of which parameters most affect the output variance due to input variability (van Griensven *et al.,* 2002) which reduces uncertainty and provides parameter estimation guidance for the calibration step of the model. SWAT model has an embedded tool to perform sensitivity analysis and provides recommended ranges of parameter changes. SWAT2005 uses a combination of Latine Hypercube Sampling and One-At-a-Time sensitivity analysis methods (LH-OAT method) (van Griensven, 2005). The concept of the Latin-Hypercube Simulation is based on the Monte Carlo Simulation to allow a robust analysis but uses a stratified sampling approach that allows efficient estimation of the output statistics while the One-Factor-At-a-Time is an integration of a local to a global sensitivity method (van Griensven, 2005). In local methods, each run has only one parameter changed per simulation which aides in the clarity of a change in outputs related directly to the change in the parameter altered (van Griensven and Green, 2007).

2.3.7. Model calibration

There are three calibration approaches widely used by the scientific community. These are the manual calibration, automatic calibration and a combination of the two. Manual calibration is the most widely used approach. However it is tedious, time consuming, and success of it depends on the experience of the modeler and knowledge of the watershed being modeled (Eckhardt & Arnold, 2001). Automatic calibration involves the use of a search algorithm to determine best-fit parameters. It is desirable as it is less subjective and due to extensive search of parameter possibilities can give results better than if done manually.

SWAT has two built-in calibration tools: the manual calibration helper and the auto- calibration. The manual calibration approach helps to compare the measured and simulated values, and then to use the expert judgment to determine which variable to adjust, how much to adjust them, and ultimately assess when reasonable results have been obtained. The auto- calibration technique is used to obtain an optimal fit of process parameters which is based on a multi-objective calibration and incorporates the Shuffled Complex Evolution Method algorithms (Green and van Griensven, 2007).

2.3.8. SWAT strength and limitation

2.3.8.1. Strength

Key features that make the model applicable for a wide range of studies are:

- Modelling based on physical processes associated with soil and water interaction
- Flexibility to incorporate crop characteristics, cropping stage and duration
- Flexibility on input data requirement
- Capability of modelling the changes in land use and management practices
- Computational efficiency
- Capability of long-term simulations
- Capability of modelling catchments areas varying between few hectares to thousands of sq.km.
- The model is freely available and can be easily downloaded from the internet

2.3.8.2. Limitation

Following are some of the limitations using SWAT for hydrological modelling:

1. Due to the heterogeneity of the catchments, a number of meteorological observation stations are required to present the spatial variation in the hydro-meteorological characteristics in the area. The lack of adequate number of observation stations affects the model output.
2. In order to calibrate the model for the historic land use scenarios, the corresponding land use maps are needed. In order to get the real time picture of the land use pattern, this information can be extracted from the remote sensing satellite imageries by using digital image processing technique. However, acquisition of satellite imageries is expensive and also the expertise required for the image interpretation is another major limitation.
3. Though SWAT is a free software tool, in order to represent the spatial variation in the catchments characteristics, GIS software is the pre-requisite to run the model.

2.3.9. RAINBO homogeneity test

Frequency analysis of rainfall data and flow data and their potential use in agrometeorolgical decision-making processes requires that the data be of long series; they should be homogeneous and independent. The restrictions of homogeneity assure that the observations are from the same population. In RAINBOW the test for homogeneity is based on the cumulative deviation from the mean and determined from equation 20.

$$D_k = \sum_{i=1}^{k} (Y_i - \overline{Y}) \qquad k= 1, 2,\ldots\ldots, n \qquad 20$$

Where Y_i are records of the partial duration series Y_1, Y_2 ….. Y_n and $\overline{Y}$ is the mean. Note that D_0 and D_n are equal to zero. For a homogeneous record one may expect that the D_k fluctuate around zero since there is no systematic pattern in the deviations of the Y_i 's from their average value. Rescaled cumulative deviations are obtained by dividing the D_k s by the sample standard deviation value S_y and then the values of the (D_k / S_y)'s are plotted. A statistical formula which is sensitive to departures from homogeneity may be written as under:

$$Q = \max\left|D_k / S_y\right| \quad 0 \le \mathrm{k} \le \mathrm{n} \tag{21}$$

$$R = \max\left|D_k / S_y\right| - \min\left|D_k / S_y\right| \tag{22}$$

High values of Q or R are an indication that the data of the time series is not from the same population and that the fluctuations are not purely random. Critical values for the test-statistic which test the significance of the departures from homogeneity are plotted in the homogeneity plot menu as well (3 horizontal lines). If the cumulative deviation crosses one of the horizontal lines the homogeneity of the data set is rejected with respectively 90, 95 and 99% probability. The probability of rejecting the homogeneity of the data set is reported in the Homogeneity statistics menu. The menu is displayed by clicking on the 'Statistics' button in the Homogeneity plot menu. If as a result of a homogeneity test, the homogeneity of the data set is rejected, the user can restrict the analysis to the fraction of the time series which is homogenous. By selecting Restrict analysis in the Main menu the user can specify the restricted time series.

3. MATERIALS AND METHODS

3.1. Description of the Study Area

The Ija Galma Waqo spate irrigation is located in Oromia Region, Eastern Harergie Zone, Fedis District and Qufa Bobasa peasant association at $9^0$01' 15" N and 42^0 12' 13" E. The catchment area covers 42.09 km^2 (Figure 1). The project is designed to supplement irrigation water for around 350 ha by the flood coming from the catchment, the main stream has a total length of 13 km. Mean elevation of the watershed is 1698.5 m with maximum of 1967 m and minimum of 1529 m above sea level. About 96.03% of the watershed has a slope $\leq$ 10% The lowest point is located at headwork site 1529 m and the highest point is the Bilalo ridge (1967 m above sea level). Close to 50.16% of the watershed area lies below 1767 m elevation and the rest above 1767 m. The watershed is generally classified as cool sub-humid "Weina Dega". Based on the meteorological data of Bisidimo, the project area has mean annual precipitation of 689.28 mm with annual maximum and minimum daily temperature of 26.44 and 12.97^{o}C, respectively.

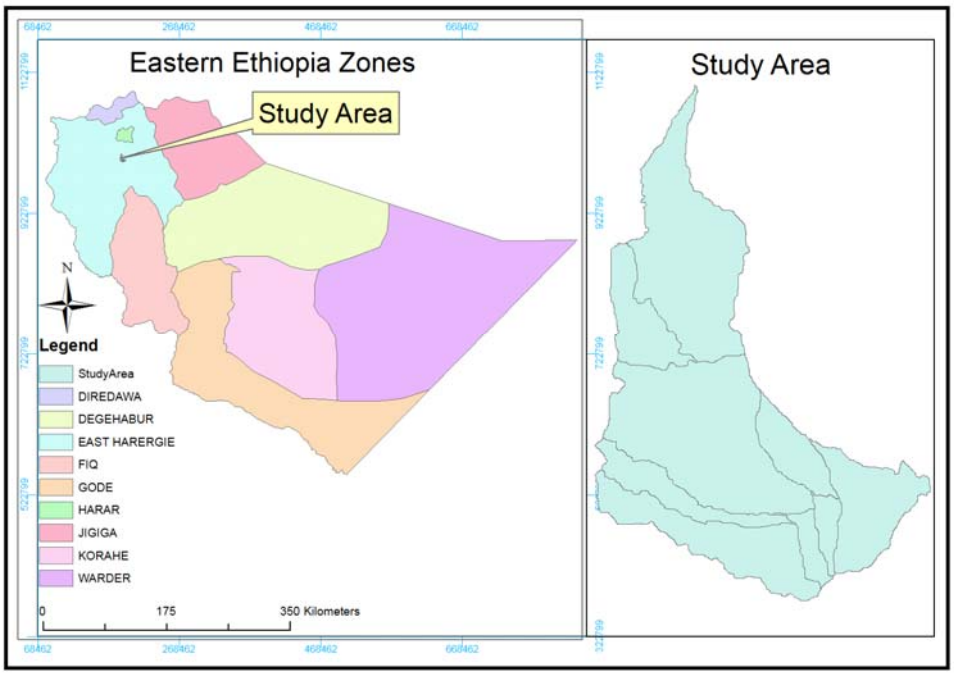

Figure 1. Location of the study area

3.2. SWAT Input

Input for SWAT is defined at several levels of detail: watershed, subbasins, or HRU. Unique features such as reservoirs or point sources must have input data provided for each individual feature included in the watershed simulation.

The Watershed level inputs are used to model processes throughout the watershed. For example, the method selected to model potential evapotranspiration will be used in all HRUs in the watershed. The subbasin level inputs are inputs set at the same value for all HRUs in the subbasin if the input pertains to a process modeled in the HRU. Because there is one reach per subbasin, input data for main channels is defined at the subbasin level also. An example of subbasin level data is rainfall and temperature information. The same rainfall and maximum and minimum temperature are used for all HRU, the main channel and any ponds or wetlands located within the subbasin. HRU level inputs are inputs that can be set to unique values for each HRU in the watershed. An example of an HRU input is the management scenario simulated in an HRU. Generally the following input data were used to analyze the sediment and runoff yield of this watershed:

3.2.1. Digital elevation model (DEM) of the study area

The topography is defined by DEM that describes the elevation of any point in a given area at a specific spatial resolution. DEM was derived from the NASA 90-meter Shutter Topography Radar Mission (STRM) dataset. It was obtained from GIS section of Haramaya University. This DEM was used to delineate the watershed and analyze the drainage pattern of the land surface terrain. Subbasin parameters such as slope gradient, slope length of the terrain and the stream network characteristics such as canal slope length and width were derived from DEM. The DEM data was processed from STRM dataset shown in Figure 2. It had a resolution of 90m and was provided in mosaic 5 deg x 5 deg tiles. Before the DEM data was loaded into Arc SWAT interface, it was projected into projected coordinate system. The projection of the DEM data was done using the Arc tool box operation in ArcGIS. The projected coordinate system parameters of study area are: UTM— other GCS—Adindan UTM zone 38N.prj.

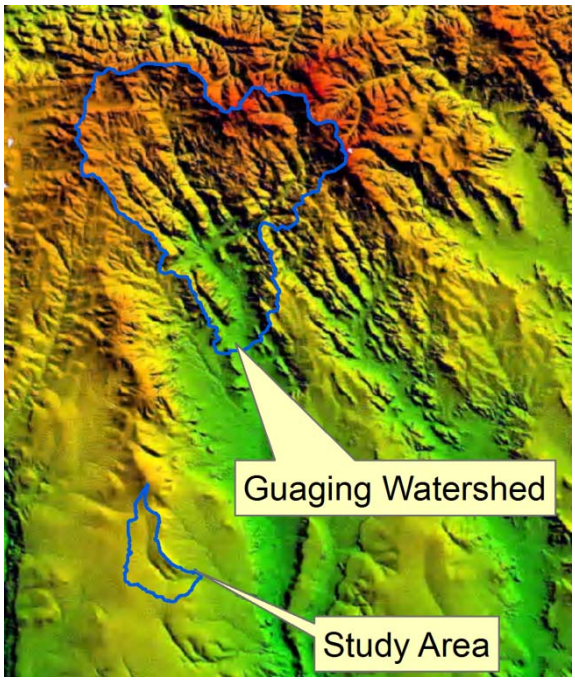

Figure 2. STRM dataset for the study area

As the STRM dataset covered a larger area in which part of it was not required for the modeling work but reduced the processing time of the GIS functions, a mask was created for the study area. Hence, only the portion of the DEM covered by the mask was processed by the interface.

3.2.2. Stream network

The stream network data set was digitized from topographic map of scale (1:50000 and 1:250000) of the study area. The digitized stream network was in a shape file format as shown in Figure 3. The stream network dataset was superimposed onto the DEM to define the location of the stream network. Burning-in stream network operation is most important in situations where the DEM does not provide enough detail to allow the interface to accurately predict the location of the stream network.

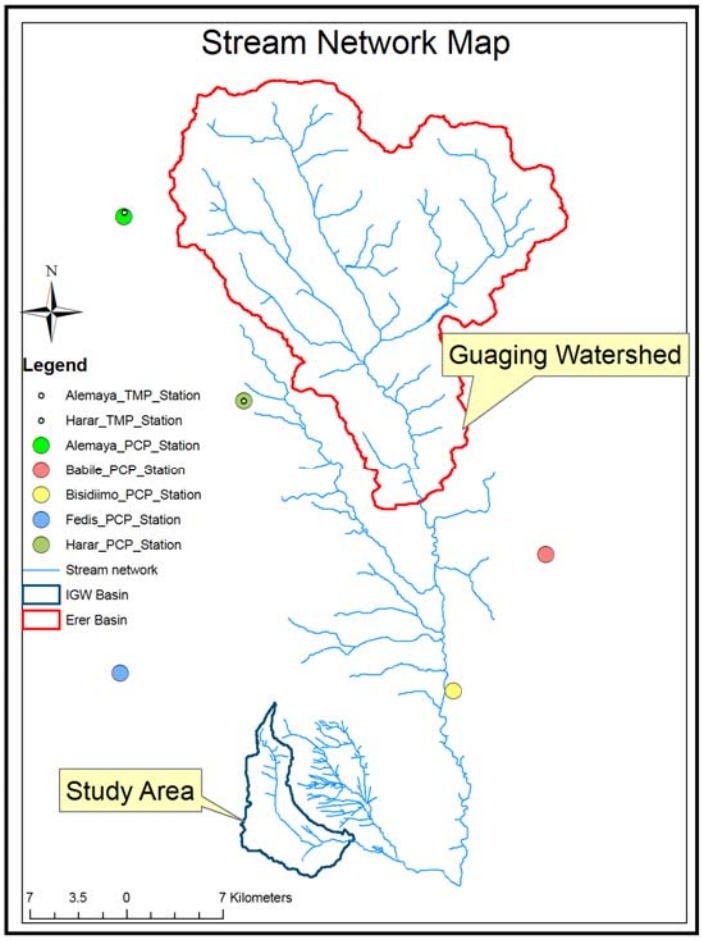

Figure 3. Stream network map in the study area

3.2.3. Land use/Land cover

The land use is one of the most important factors that affect runoff, evapotranspiration and surface erosion in a watershed. The land use map of the study area was obtained from Ministry of Water Resources from the study of Wabisheble river basin and field observation. The reclassification of the land use map was done to represent the land use according to the specific land cover types and the respective crop parameter was selected from SWAT database. A look up table that identifies the 4-letter SWAT code for the different categories of land cover/land use were prepared so as to relate the grid values to SWAT land cover/land use classes. SWAT calculated the area covered by each land use. The different land use/cover types are presented in Table 1.

Table 1. Land use/ land cover types in the study area and corresponding SWAT value

Original land use	Corresponding SWAT Definition	SWAT Code
Maize	Corn	CORN
Sorghum	Grain Sorghum	GRSG
Open Grass	Range grass	RNGE
Open shrub	Range-brush	RNGB

3.2.4. Soil data

The SWAT model requires different soil textural and physical-chemical properties such as soil texture, available water content, hydraulic conductivity, bulk density and organic carbon content for different layers of soil. These data were obtained mainly from the following sources: Wabishebele river basin Soil database and digital soil map from the Ministry of Water Resource. Physical soil property calculator was used to calculate the available soil moisture content, bulk density and saturated hydraulic conductivity and the default Value of the model. Whereas the soil erodibility (K) factor was calculated according to Williams (1995) by using equation 20

$$K_{USLE} = f_{csand} \cdot f_{cl-si} \cdot f_{orgc} \cdot f_{hisand} \quad 23$$

Where f_{csand} is a factor that gives low soil erodibility factors for soils with high coarse-sand contents and high values for soils with little sand, $f_{cl\text{-}si}$ is a factor that gives low soil erodibility factors for soils with high clay to silt ratios, f_{orgc} is a factor that reduces soil erodibility for soils with high organic carbon content, and f_{hisand} is a factor that reduces soil erodibility for soils with extremely high sand contents. The factors are calculated by using equation 21 to 24.

$$f_{csand} = \left(0.2 + 0.3 \cdot \exp\left[-0.256 \cdot m_s \cdot \left(1 - \frac{m_{silt}}{100}\right)\right]\right) \quad 24$$

$$f_{cl-si} = \left(\frac{m_{silt}}{m_c + m_{silt}}\right)^{0.3} \quad 25$$

$$f_{orgc} = \left(1 - \frac{0.25 \cdot orgC}{orgC + \exp[3.72 - 2.95 \cdot orgC]}\right) \quad 26$$

$$f_{hisand} = \left(1 - \frac{0.7 \cdot \left(1 - \frac{m_s}{100}\right)}{\left(1 - \frac{m_s}{100}\right) + \exp\left[-5.51 + 22.9 \cdot \left(1 - \frac{m_s}{100}\right)\right]}\right) \quad 27$$

Where m_s is the percent sand content (0.05-2.00 mm diameter particles), m_{silt} is the percent silt content (0.002-0.05 mm diameter particles), m_c is the percent clay content (< 0.002 mm diameter particles), and *orgC* is the percent organic carbon content of the layer (%).

3.2.5. Meteorological data

Meteorological data is needed by the SWAT model to simulate the hydrological conditions of the basin. The meteorological data required for this study were collected from the Ethiopian National Meteorological Services Agency (NMSA) and MoWR. The meteorological data collected were precipitation, maximum and minimum temperature, relative humidity, and wind speed and sunshine hours. Data from six stations, which are within and around the study area, were collected. For Haramaya station records between 1981 and 2005 were obtained. However for the rest of the stations, climatic records during the years 1994 to 2008 were obtained. But most of them have missing data especially during 1991-1992 (during government transition in Ethiopia). The other problem in the weather data was inconsistency in the data record, in some periods there is a record for precipitation but temperature data are missing, and vice versa.

For this study the selected weather generator stations (station used for infilling of missing data) were Harar, and Haramaya stations due to the availability of data, closeness to the project and quality of data. They are class A meteorological stations. Moreover to estimate the representative rainfall we used the nearest meteorology stations such as Fedis, Besidimo and Babile as an input for rainfall and Haramaya and Harar for temperature. The rainfall and temperature data of at least 10 years were collected from the Ethiopian Meteorology Agency, wind speed and relative humidity from MoWR, the solar radiation was computed using Climwat2 software, and the dew point temperature was computed by equation 27.

The saturation vapor pressure e_s was derived from the daily air temperature values T (equation 25). After that, the actual average daily vapor pressure e_a was calculated using saturation vapor pressure e_s and average humidity data (RH) equation 26. According to Allen, (1998):

$$e_s = 0.6108 * \exp((1\ 7.27 * T) / (T + 237.3)) \quad 28$$

The unit for saturation vapor pressure generated by equation 25 is [kPa] and Kpa * 10 is equal to mbar. According to Hackel, (1999):

$$e_a = RH*e_s/100 \quad 29$$

The daily dew point temperature was calculated using equation 27.

$$Dew = (234.18 * 1\log_{10}(e_s) - 184.2)/ (8.204 - \log_{10}(e_s)) \quad 30$$

Where Dew = dew point temperature [°C], e_s = saturation vapour pressure [mbar], e_a = actual vapor pressure [mbar], exp = 2.7183 (base of natural logarithm), T = air temperature [°C] and RH = relative humidity [%].

Using daily minimum and maximum temperature data, the saturation vapor pressure were derived twice (e_{smin} and e_{smax} according to equation 25. In this case the saturation vapour pressure used by equation 26 was the mean value of e_{smin} and e_{smax}.

This weather generator input file contains the statistical data needed to generate representative daily climate data for the subbasins. Climatic data was generated in two instances: when the user specific that simulated weather could be used or when measured data was missing. The weather generator inputs are presented in Appendix I.

3.2.6. Hydrological data

The hydrological data was required for performing sensitivity analysis, calibration and uncertainty analysis and validation of the model. The hydrological data was also collected from

the Ethiopian MoWR hydrology section. The hydrological data collected was daily flow for the Erer rivers feeding into Wabishebele river. It was the only hydrological data used for sensitivity analysis, calibration and validation. The homogeneity of average annual daily flow data was tested using RAINBO software. In a frequency analysis estimates of the probability of occurrence of future rainfall (or flows) events are based on the analysis of historical rainfall (or flows) records. Frequency analysis of data requires that the data be homogeneous and independent. The restriction of homogeneity assures that the observations are from the same population. By assuming that the past and future data sets are stationary and have no apparent trend one may expect that future time series will reveal frequency distributions similar to the observed one. RAINBO software package uses as inputs the historic event record of the data to be tested.

3.3. Arc SWAT Model Setup

Geographic information systems data for the SWAT model were preprocessed by two separate functions watershed delineation and determination of hydrologic response units (HRUs) and outlined in the next subtopics in detail:

3.3.1. Watershed delineation

Arc SWAT uses Digital Elevation Model (DEM) data to automatically delineate the watershed into several hydrologically connected sub-watersheds. The watershed delineation operation uses and expands ArcGIS and Spatial Analyst extension functions to perform watershed delineation. The first step in the watershed delineation was loading the properly projected DEM. To reduce the processing time of the GIS functions, a mask was created over the DEM around the study area. Next, a polyline stream network dataset was burnt-into force SWAT sub-basin reaches to follow known stream reaches. Burning-in a stream network improves hydrological segmentation, and sub-watershed delineation. After the DEM grid was loaded and the stream networks superimposed, the DEM map grid was processed to remove the non draining zones.

The initial stream network and sub-basin outlets were defined based on drainage area threshold approach. The threshold area defines the minimum drainage area required to form the origin of a stream. The interface lists a minimum, maximum and suggested threshold area. The smaller the

threshold area, the more detailed the drainage network delineated by the interface but the slower the processing time and the larger memory space required. In this study, defining of the threshold drainage area was done using the threshold value. Besides those sub-basin outlets created by the interface, outlets were also manually added at the gauging stations where sensitivity analysis, calibration and validation tasks were later performed. Then watershed delineation activity was finalized by calculating the geomorphic sub-basin parameter.

3.3.2. Hydrologic response unit analysis

Hydrologic response units (HRUs) are lumped land areas within the sub-basin that are comprised of unique land cover, soil, slope and management combinations. HRUs enable the model to reflect differences in evapotranspiration and other hydrologic conditions for different land covers and soils. The runoff is estimated separately for each HRU and routed to obtain the total runoff for the watershed. This increases the accuracy in flow prediction and provides a much better physical description of the water balance.

The land use and the soil data in a projected Grid file format were loaded into the ArcSWAT interface to determine the area and hydrologic parameters of each land-soil category simulated within each sub-watershed. The land cover classes were defined using the look up table. A look-up table that identifies the 4-letter SWAT code for the different categories of land cover/land use was prepared so as to relate the grid values to SWAT land cover/land use classes. After the land use SWAT code assigned to all map categories, calculation of the area covered by each land use and reclassification were done. As of the land use, the soil layer in the map was linked to the user soil database information by loading the soil look-up table and reclassification applied. The land slope classes were also integrated in defining the hydrologic response units. The DEM data used during the watershed delineation was also used for slope classification. The multiple slope discretization operation was preferred over the single slope discretization as the sub-basins have a wide range of slopes between them. Based on the suggested minimum, maximum, mean and median slope statistics of the watershed, three slope classes (0- 10, 10-20, and >20) were applied and slope grids reclassified. Then land use, soil and slope grids were overlaid.

The last step in the HRU analysis was the HRU definition. The HRU distribution in this study was determined by assigning multiple HRU to each sub-watershed. In multiple HRU definition, a threshold level was used to eliminate minor land uses, soils or slope classes in each sub-basin. Land uses, soils or slope classes which cover less than the threshold level were eliminated and the area of the remaining land use, soil, or slope class was reapportioned so that 100% of the land area in the sub-basin was modeled. The threshold levels set is a function of the project goal and amount of detail required. In the SWAT user manual it is suggested that it is better to use a larger number of sub-basins than larger number of HRUs in a sub-basin; a maximum of 10 HRUs in a sub-basin is recommended. Hence, taking the recommendations in to consideration, 5%, 5%, and 5% threshold levels for the land use, soil and slope classes were applied, respectively so as to encompass most of spatial details.

3.3.3. Importing climate data

The climate of a watershed provides the moisture and energy inputs that control the water balance and determine the relative importance of the different components of the water cycle. The climatic variables required by SWAT daily precipitation, maximum and minimum temperature, solar radiation, wind speed and relative humidity were prepared in the appropriate dbase format. Due to data availability and quality, daily precipitation, and maximum and minimum temperature in dbase format were the climatic input variables imported together with their weather location. And due to lack of complete weather data we used the Hargreaves method which uses Temperature to determine the potential evapotranspiration.

3.3.4. Sensitivity analysis

The sensitivity analysis of this study was done using Latine Hypercube Sampling and One-At-a-Time sensitivity analysis methods. The inputs were the observed daily flow data, the simulated annual flow in period (1983-1991) and the sensitive parameter in relation to flow with the absolute lower and upper bound and default type of change tobe applied (method application) used.

3.3.5. Model calibration

Even though the target of this study was not to calibrate the model, the hydrologic component of the model was calibrated at Erer gauging station in order to make the simulation result more realistic for independent calibration period (1988 to 1991).

In this study, both the manual and auto-calibration techniques were employed to get the best model parameters.

First, the manual calibration was performed and when the model evaluation parameters reached to an unchanged level, the model was run automatically. Parameter changes in SWAT affecting hydrology were done in a distributed way for selected sub-basins and HRU's. They were modified by replacement, by addition of an absolute change and by multiplication of a relative change depending on the nature of the parameter. However, a parameter has never been allowed to go beyond the predefined absolute parameter ranges during the calibration process. In the manual calibration, first the water balance was calibrated followed by temporal flow calibration. The procedure followed for calibrating the SWAT model is shown in Figure 4.

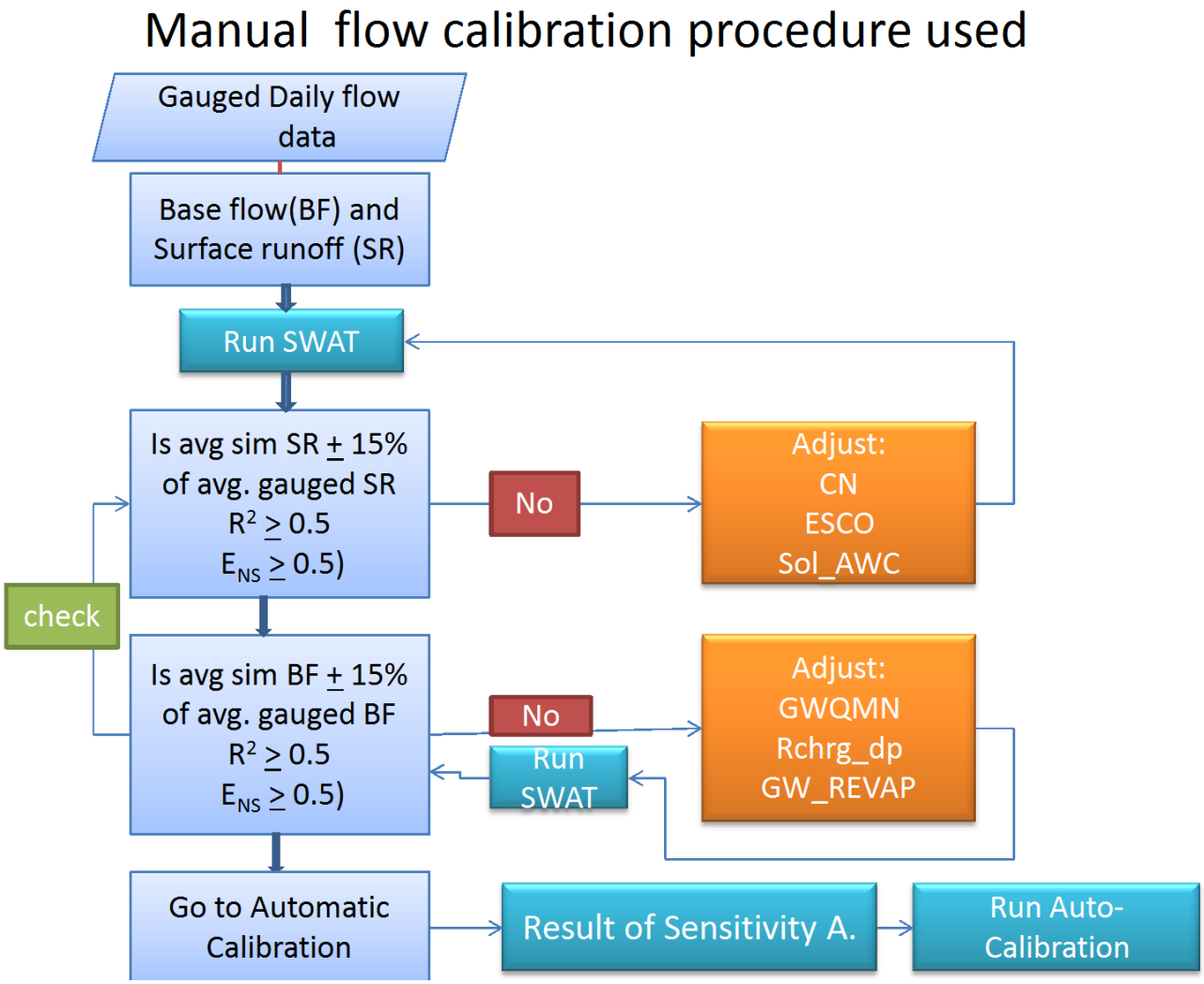

Figure 4. Calibration procedure for flow

Calibration for the water balance was done first for average annual conditions. Once the run was calibrated for the average annual conditions, calibration for average monthly was performed to fine-tune the calibration. The calibration was done separately for the surface runoff and base-flow as the parameters affecting them were different. A base-flow filter program was used to determine the relative proportion of annual flow contribution from surface runoff or base-flow. After the base flow and surface runoff were separated, the surface runoff was calibrated by adjusting the sensitive parameters which affect surface runoff like Cn2 (Initial SCS runoff curve number for moisture condition II), Ch_N (Manning's "n" value for the main channel) and Esco (Soil evaporation compensation factor). The simulated versus observed values for each adjustment were evaluated with coefficient of determination (R^2) and Nash-Sutcliffe efficiency

(E_{NS}). When the values of R^2 and E_{NS} were above 0.5, calibration of base-flow was followed. Base-flow calibration was performed by adjusting the sensitive parameters which affects groundwater contribution. The most sensitive base-flow parameters which were adjusted were GW_Revap (Groundwater "revap" coefficient), REVAPMN (threshold depth of water in the shallow aquifer for "revap" or percolation to occur), and GWQMN (depth of water in the shallow aquifer required for return flow to occur). Like surface runoff calibration, the simulated versus observed values were evaluated with R^2 and E_{NS}. The parameters were adjusted until the R^2 and E_{NS} results were above 0.5. However; after adjustments of base-flow parameters, the surface runoff was checked because the adjustments of the base-flow parameters will affect the surface runoff in some way.

Once the water balance was calibrated, temporal flow calibration was performed at each step by adjusting parameters which affects the shape of the hydrograph. The parameters adjusted were Ch_K (effective hydraulic conductivity in main channel alluvium), alpha_BF (baseflow alpha factor), Surlag (Surface runoff lag coefficient) and GW-Delay (Groundwater delay time).

After the parameters were manually calibrated and were reached to acceptable value as per the R^2 and E_{NS}, the final parameter values that were manually calibrated were used as the initial values for the auto-calibration procedure. Maximum and minimum parameter value limits were used to keep the output values within a reasonable value range. Finally, the auto calibration tool was run to provide the best fit between the measured and simulated data.

3.3.6. Model validation

In order to utilize the calibrated model for estimating the effectiveness of future potential management practices, the model was tested against an independent set of measured data. This testing of a model on an independent set of data set was used. As the model predictive capability was demonstrated as being reasonable in both the calibration and validation phases, the model was used for future predictions under different management scenarios. In this study, the model was validated with independent validation period (1984-1987).

3.4. Model Evaluation

The performance of SWAT was evaluated using statistical measures to determine the quality and reliability of predictions when compared to observed values. Coefficient of determination (R^2) and Nash-Sutcliffe simulation efficiency (E_{NS}) were the goodness of fit measures used to evaluate model prediction. The R^2 value is an indicator of strength of relationship between the observed and simulated values. The Nash-Sutcliffe simulation efficiency (E_{NS}) indicates how well the plot of observed versus simulated value fits the 1:1 line. If the measured value is the same as all predictions, E_{NS} is 1. If the E_{NS} is between 0 and 1, it indicates deviations between measured and predicted values. If E_{NS} is negative, predictions are very poor, and the average value of output is a better estimate than the model prediction (Nash and Sutcliffe, 1970). The R^2 and E_{NS} values are explained in equations 28 and 29 respectively.

$$R^2 = \frac{\left(\sum_{i=1}^{n} (O_i - Oav)(P_i - P_{av}) \right)^2}{\sum_{i=1}^{n} \left(O_i - O_{av} \right)^2 \sum_{i=1}^{n} \left(P_i - O_{av} \right)^2} \qquad 31$$

$$E_{NS} = \frac{\sum_{i=1}^{n} \left(O_i - O_{av} \right)^2 - \sum_{i=1}^{n} \left(P_i - O_{av} \right)^2}{\sum_{i=1}^{n} \left(O_i - O_{av} \right)^2} \qquad 32$$

Where n is the number of observations during the simulation period O_i and P_i are the observed and predicted values at each comparison point i, O_{av} and P_{av} are the arithmetic means of the observed and predicted values.

4. RESULT AND DISCUSION

4.1. Model Setup

4.1.1. Catchments characteristics of Ija Galma Waqo and Erer gauging station

The watershed delineation and HRU definition in the Ija galma Waqo diversion point and Erer gauging station gave watershed areas of 42.09 km^2 and 488.55 km^2 which resulted in 9 and17 sub-basins with 27 and 120 HRUs, respectively. The area coverage by each land use type is presented in Table 2 and Figure 5.

Table 2. Land use type and their area coverage in study area

Watershed	Land Use	SWAT code	Area (km^2)	% of total area
Erer gauging station	Maize	CORN	476.70	97.57
	Open shrubs	RNGE	11.85	2.43
Ija Galma Waqo	Range brush	RNGE	7.27	17.28
	Grain Sorghum	GRSG	34.82	82.72

As it was observed in Table 2 and Figure 5 in both watersheds, most portion of the watershed is covered with Maize and sorghum, which accounts for 97.57 and 82.72 % of their respective watershed area. The value of the land use presented in the Table 2 was after the definition of HRU but the figure 5 was inputs before the definition, for that reasons they are different.

The soil types of both watersheds is presented in Table 3 and Figure 6, it was shown that there are two types in Ija Galma Waqo watershed and five types in the Erer gauging station. The dominant soil type in both watersheds is Chromic Luvisoil. The detail parameter values are presented in Appendix III.)

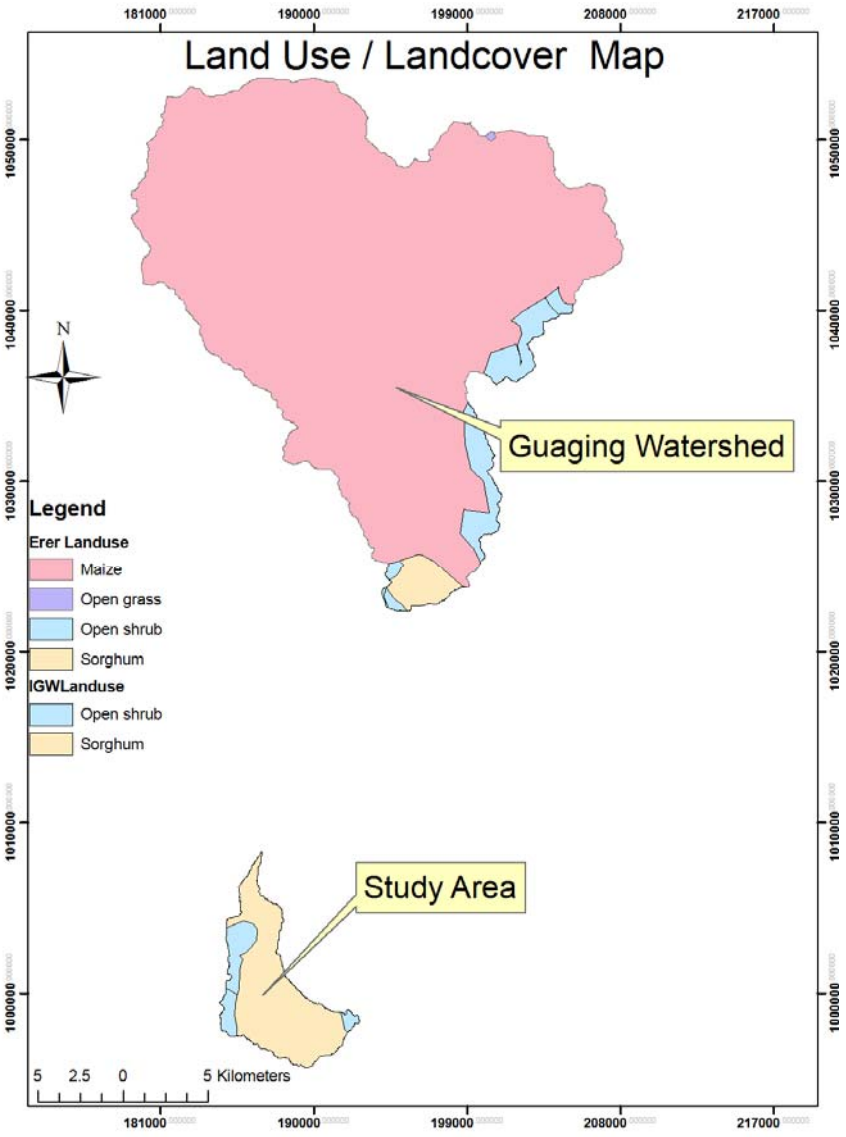

Figure 5. Land use / Land cover map of the study area

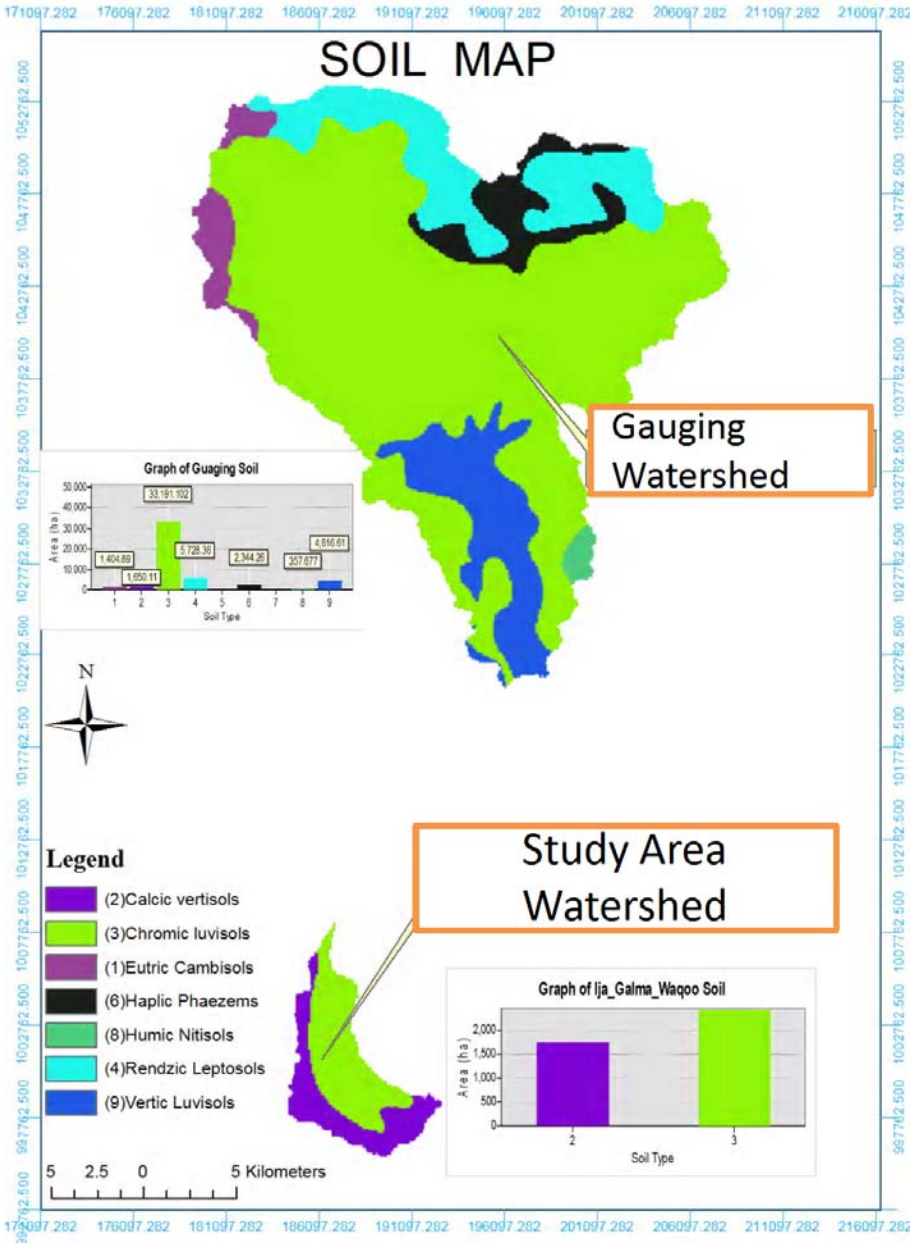

Figure 6. Soil map of the study area

As shown in Table 3, 96.65% of the area in Ija Galma Waqo had a slope less than 10% while 43.23% of the area in Erer gauging station had a slope greater than 20%. The value of the soil presented in the Table 3 was after the definition of HRU but the figure 6 was inputs before the definition, for that reasons they are different

Table 3. Soil type and slope classes and their areal coverage

Ija Galma Waqo	Soil type		Area (km^2)	% of total area
	Calcic Vertisol		17.49	41.57
	Chromic Luvisol		25.59	58.43
	Slope	< 10%	40.68	96.65
		10-20%	1.4	3.35
Erer gauging station	Soil type		Area (km^2)	% of total area
	Chromic Luvisol		340.31	69.66
	Eutric Cambisol		13.97	2.86
	Rendzinc Leptosol		62.89	12.87
	Haplic Phaezems		24.79	5.47
	Vertic Luvisol		46.58	9.54
	Slope	<10%	124	25.38
		10-20%	153.35	31.39
		>20%	211.19	43.23

The weather data used for the study was set from 1983-2008 of which 1983-1991 was for Erer gauging station and 1994-2008 for Ija Galma Waqo project. The homogeneity of the annual rainfall was tested for all stations using RAINBO software.

The result of homogeneity test for the weather generator and observed gauging stations data shows that the collected data was homogeneous except for Harar which is rejected at 90 % . This was due to the maximum cumulative deviation crosses the 90 % probability line. The estimated change point was the record of annual rainfall 616 mm in 2000. The test result for Haramaya station was presented in Table 4, Figure 7 and Figure 8. Details are presented in the Appendix II.

Homogeneity Test of annual rainfall for Haramaya station

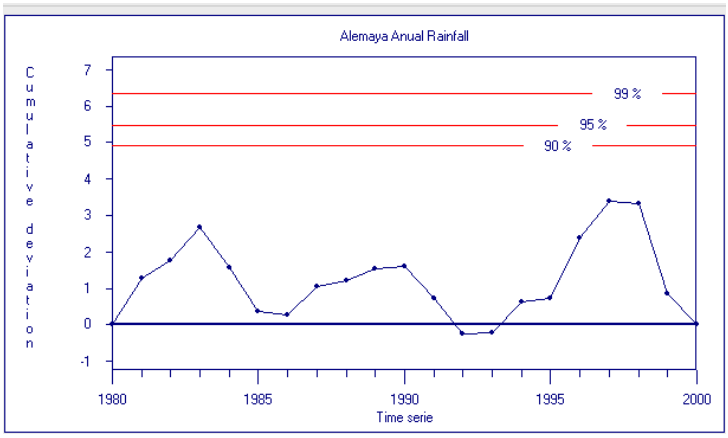

This graph was used to determine the position of change points. At points where the cumulative deviation sum plot shows a clear change in slope, it is assumed that there is a change in trend estimates of change point (year) is 1997

Figure 7. Rescaled cumulative deviation of annual rainfall at Haramaya station

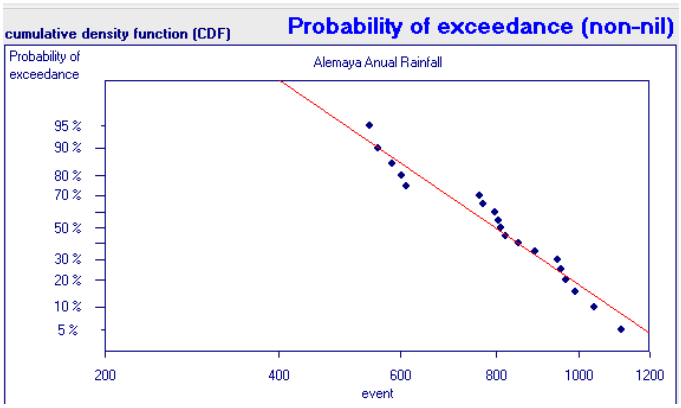

The probability plot of annual rainfall is given Appendix Figure A.2. The least square fit R^2 is 0.97

Figure 8. Probability plot of annual rainfall at Haramaya Station

Table 4. Probability of rejecting homogeneity of annual rainfall (Haramaya station)

Statistics	Rejected?		
	90%	95%	99%
Range of Cumulative deviation	No	No	No
Maximum Cumulative deviation	No	No	No

Closeness of linear relationship (CDF) R^2 =0.97

4.1.2. Sensitivity analysis

Results of sensitivity analysis with observed data showed that most sensitive parameters for the SWAT model in Erer sub-watershed are base flow alpha factor (Alpha_Bf), curve number (Cn2), soil evaporation compensation factor (Esco), maximum canopy storage (Canmx), plant uptake composition factor (Epco), available water capacity (Sol_Awc), effective hydraulic conductivity in main canal (Ch_k2), saturated hydraulic conductivity of soil (Sol_k), biological mixing efficiency (Biomix) and manning's roughness in main canal (Ch_N). The top ten sensitive parameters which have effect on the runoff along with their ranking and their method of adjustment are presented in Table 5.

Table 5. Sensitive parameter ranking and final auto-calibration result

		Bound		Aut-calibration result	
Parameter	Rank	Lower	Upper	Fitting Value	Method
Alpha_Bf	1	0	1	0.49	replace
Cn2	2	-25	25	1.0091	multiply
Esco	3	0.01	1	0.1	replace
Canmx	4	0	100	0.14	replace
Epco	5	0.01	1	0.23	replace
Sol_Awc	6	-10	10	1.01	multiply
Ch_K2	7	0	150	0.38	replace
Sol_K	8	-10	10	1.0023	multiply
Biomix	9	0	1	0.93	replace
Ch_N	10	0	0.3	0.3	replace

4.1.3. Model calibration

The auto calibration run of 5000 iteration resulted as Table 5 last columns the value was used to calibrate the model parameter in a distributed way for the gauging and study area. The result of simulation was evaluated with the observed and found to have $R^{2} =$ 0.64 and E_{NS} = 0.56 for the calibration period as shown in Figure 9.

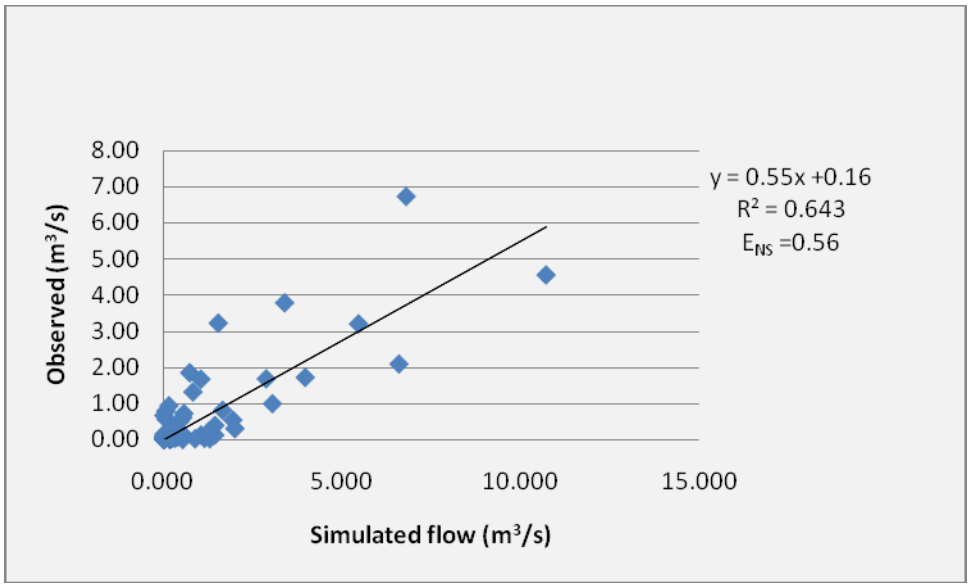

Figure 9. Comparison between observed and simulated stream flow for calibration period

Table 6. Calibration and validation period statistics for measured and simulated flows

Period	Average flow (m^3/s)		error
	Observed	Simulated	
Calibration(1988-1991)	1.36	0.86	0.36
Validation(1984-1987)	0.484	0.578	0.19

Figure 10 shows that the simulated flows can represent the observed flows except that the peak values couldn't be caught. This might be due to the fact that greater attention was paid for the water balance calibration than shape of the hydrograph.

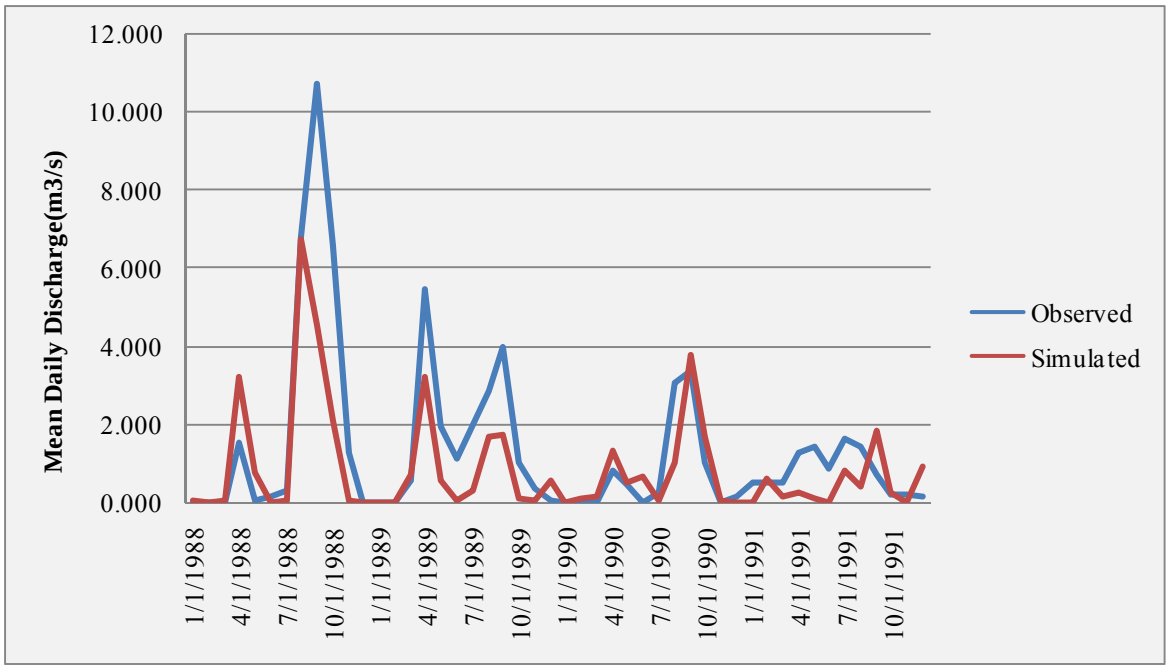

Figure 10. Observed and simulated flow hydrograph for calibration period

4.1.4. Model validation

Validation of the model was done for an independent data set of four years from 1984 to 1987. It was found that the model has strong predictive capability with R^2 and E_{NS} value of 0.73 and 0.5, respectively. It can be seen from Figures 11 and 12 that the model simulates the observed flow well. However it couldn't catch the peak flows.

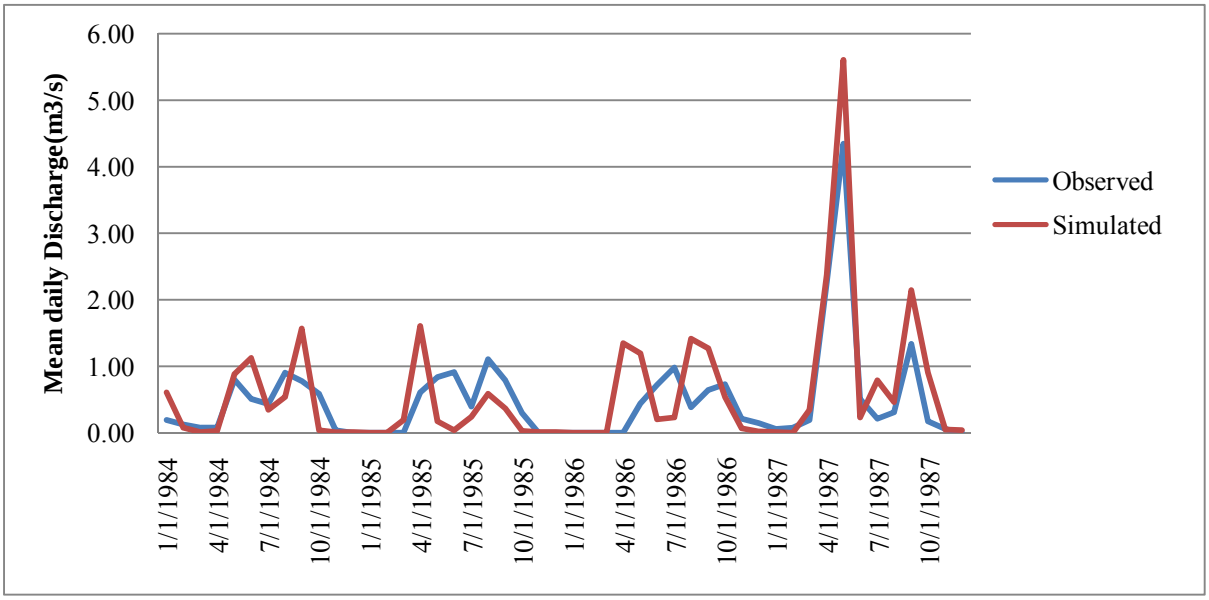

Figure 11. Observed and simulated flow hydrograph for validation period

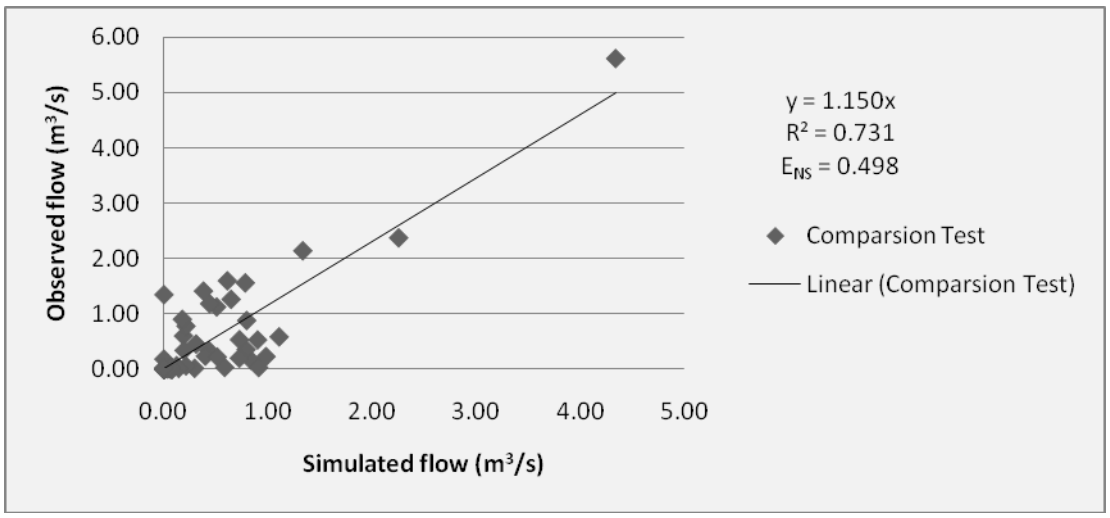

Figure 12. Comparison between observed and simulated stream flow for validation period

4.2. Ija Galma Waqo Water and Sediment Yield Simulation

4.2.1. The water yield

Water and sediment yield were simulated using the land cover and soil type data in Table 2 and 3 and with the daily rainfall and minimum and maximum temperature collected from Bisidimo and

Fedis meteorological stations. These stations are selected by the model due to their closeness to the area of interest.

The water yield was simulated for the year 1994 to 2008 on monthly time step. The result was summarized as Intermediate (Feb-May), Wet (Jun-Sep), Dry (Oct-Jan) and yearly basis, after calibration of sensitive parameters for flow obtained during the auto-calibration of Erer gauging station. The result is shown in Table 7, Table 8 and Table 10.

Table 7. Simulated monthly water yield (ha-m) at diversion point

	Month												Total
Year	Jan	Feb	Mar	Apr	May	Jun	Jul	Aug	Sep	Oct	Nov	Dec	
1994	0.0	0.0	0.0	0.0	0.0	0.3	1.3	2.0	15.0	2.3	2.9	0.1	23.90
1995	0.0	0.0	6.5	62.7	28.5	2.7	32.5	12.0	23.0	0.3	0.2	0.1	168.50
1996	0.1	0.1	41.3	97.2	159.1	262.2	15.2	67.8	26.6	0.7	1.8	0.2	672.30
1997	0.1	0.1	2.5	13.2	0.7	0.5	51.9	3.5	0.1	258.1	101.7	2.2	434.60
1998	20.8	19.4	3.1	3.1	15.4	0.5	0.2	0.1	35.5	55.0	0.3	0.1	153.50
1999	0.1	0.0	74.3	0.3	2.7	0.1	0.1	9.3	24.2	23.6	0.5	0.2	135.40
2000	0.1	0.1	0.1	18.3	102.7	2.8	0.1	143.8	17.6	10.7	24.6	0.1	321.00
2001	0.1	0.1	13.3	19.0	7.7	4.6	0.3	4.7	0.4	0.1	0.1	0.0	50.40
2002	0.0	0.0	7.2	9.1	0.3	11.7	6.3	29.5	5.9	5.7	0.1	0.1	75.90
2003	9.5	0.1	0.0	106.2	6.4	0.1	3.5	0.6	57.4	0.1	0.1	3.2	187.20
2004	0.1	0.0	0.0	13.8	0.1	0.1	0.1	0.1	0.1	0.1	0.5	0.1	15.10
2005	0.1	0.0	0.0	1.2	0.3	0.1	0.1	0.1	1.1	0.9	0.1	0.0	4.00
2006	0.0	0.0	0.0	8.5	0.1	0.1	0.1	0.3	0.6	177.2	10.6	0.2	197.70
2007	0.1	0.1	2.2	55.8	11.2	5.9	0.1	1.5	1.8	1.4	14.8	0.2	95.10
2008	0.1	0.1	0.1	0.8	57.3	26.7	51.9	33.7	8.0	20.9	27.8	0.2	227.60
Average	2.08	1.34	10.04	27.28	26.17	21.23	10.91	20.60	14.49	37.14	12.41	0.47	184.15

Table 8. Water yield (ha-m) for different probabilities of exceedence

Probability of Exceedance (%)	Return period (year)	Period (Time)			
		Annual	Intermediate	Wet	Dry
5	20	343.1	115.3	121.9	110.3
10	10	300.3	100.7	105	92.5
15	6.67	271.4	90.9	93.6	80.5
20	5	248.4	83	84.6	71
25	4	228.7	76.1	76.8	62.9
30	3.33	211	70	69.8	55.5
35	2.86	194.6	64.2	63.4	48.7
40	2.5	179.1	58.8	57.2	42.3
45	2.22	164.1	53.4	51.3	36.1
50	2	149.3	48.1	45.5	30
55	1.82	134.5	42.7	39.6	23.8
60	1.67	119.5	37.1	33.7	17.6
65	1.54	103.9	31.2	27.6	11.2
70	1.43	87.5	24.8	21.1	4.4
75	1.33	69.9	17.6	14.1	0
80	1.25	50.1	9	6.4	0
85	1.18	27.2	0	0	0
90	1.11	0	0	0	0
95	1.05	0	0	0	0

The average annual water yield 184.17 ha-m of water with coefficient of variability 0.97 was obtained. As shown in Table 10, the water yield for Intermediate, Wet and Dry were 64.85, 67.23 and 52.09 ha-m with their respective coefficient of variability 1.17, 1.43 and 1.89. These indicate that there was a relative variability among the seasonal yield. The annual crops are common in the study area of which sorghum is the dominant ones, the Intermediate and Wet water yield are of vital importance, therefore the 70 % dependable water yield for annual, intermediate wet and dry are 87.50, 24.80, 21.10 and 4.40 ha-m, respectively the detail for different probabilities are presented in Table 8.

Table 9. Simulated monthly sediment yield (t/ha) at diversion point

	Month												Total
Year	Jan	Feb	Mar	Apr	May	Jun	Jul	Aug	Sep	Oct	Nov	Dec	
1994	0.00	0.00	0.00	0.00	0.00	0.00	0.01	0.02	0.16	0.02	0.03	0.00	0.24
1995	0.00	0.00	0.16	0.63	0.40	0.03	0.29	0.11	0.23	0.00	0.00	0.00	1.85
1996	0.00	0.00	1.28	0.81	1.68	3.73	0.21	1.05	0.26	0.00	0.02	0.00	9.04
1997	0.00	0.00	0.10	0.22	0.01	0.00	0.40	0.02	0.00	4.39	1.45	0.02	6.61
1998	0.98	0.80	0.07	0.03	0.14	0.00	0.00	0.00	0.30	0.51	0.00	0.00	2.83
1999	0.00	0.00	2.65	0.01	0.03	0.00	0.00	0.08	0.23	0.22	0.00	0.00	3.22
2000	0.00	0.00	0.00	0.25	1.17	0.03	0.00	1.59	0.17	0.09	0.25	0.00	3.55
2001	0.00	0.00	0.37	0.24	0.05	0.04	0.00	0.04	0.00	0.00	0.00	0.00	0.74
2002	0.00	0.00	0.18	0.08	0.00	0.08	0.05	0.24	0.04	0.04	0.00	0.00	0.71
2003	0.35	0.00	0.00	1.83	0.05	0.00	0.02	0.00	0.48	0.00	0.00	0.03	2.76
2004	0.00	0.00	0.00	0.22	0.00	0.00	0.00	0.00	0.00	0.00	0.00	0.00	0.22
2005	0.00	0.00	0.00	0.01	0.00	0.00	0.00	0.00	0.01	0.00	0.00	0.00	0.02
2006	0.00	0.00	0.00	0.13	0.00	0.00	0.00	0.00	0.00	1.93	0.10	0.00	2.16
2007	0.00	0.00	0.09	0.94	0.09	0.04	0.00	0.01	0.01	0.01	0.13	0.00	1.32
2008	0.00	0.00	0.00	0.01	0.44	0.28	0.44	0.25	0.07	0.20	0.25	0.00	1.94
Average	0.09	0.05	0.33	0.36	0.27	0.28	0.09	0.23	0.13	0.49	0.15	0.00	2.48

Table 10. Summarized water and sediment yield at the diversion point

	Mean Water Yield			Mean Sediment Yield		
Period	Yield(ha-m)	SDAV	CV	Yield(t/ha)	SDAV	CV
Jan	2.09	5.73	2.74	0.09	0.26	2.96
Feb	1.36	5.01	3.69	0.05	0.21	3.87
Mar	10.06	20.7	2.06	0.33	0.72	2.21
Apr	27.28	35.69	1.31	0.36	0.51	1.4
May	26.15	46.41	1.77	0.27	0.5	1.84
Jun	21.23	67.03	3.16	0.28	0.96	3.39
Jul	10.91	18.77	1.72	0.09	0.16	1.67
Aug	20.6	38.91	1.89	0.23	0.46	2.04
Sep	14.48	16.63	1.15	0.13	0.15	1.12
Oct	37.14	76.3	2.05	0.49	1.19	2.4
Nov	12.4	26.4	2.13	0.15	0.37	2.49
Dec	0.47	0.92	1.95	0	0.01	2.7
Annual	184.17	179.17	0.97	2.48	2.49	1
Intermediate	64.85	75.94	1.17	1.01	1.08	1.07
Wet	67.23	96.2	1.43	0.73	1.34	1.82
Dry	52.09	98.67	1.89	0.73	1.54	2.09

4.2.2. Sediment yield

In this study the SWAT model which was calibrated and validated only for hydrological component of Erer gauging station was used to estimate the sediment yield with their respective distribution among the subbasins. Even though due to lack of observed data for sediment, the result of the model is indicative since the most driving force i.e. Runoff is calibrated. Based on this simulation, the annual sediment yield at the diversion point of Ija Galma Waqo project was in the range of 0.02 to 9.04 tons per hectare during the year 1994 to 2008 with annual average yield of 2.48 tons/ha and the coefficient of variation of 1.00. The detail is presented in Table 9 and Table 10.

4.2.3. Sediment distribution

The spatial variability of sedimentation rate were identified and shown in figure 13 and based on which the potential area of intervention can identified. The average annual yield of sedimentation for each subbasin was used to generate sediment source map shown in Figure 13. The output of model showed that Subbasin 6 of Ija Galma Waqo at the existing condition generates a maximum annual average sediment yield of 13.3 ton/ha, this was attributed due to the topographic slope and landuse of this subbasin. It was an agricultural land with $\geq$ 12.72% of which has a slope > 20%. And the minimum yield of less than 1.5 tons/ha was obtained for subbasin 2, it has a slope < 10% and 64.87% of it was covered by range brush the rest was agricultural.

Hurni (1989) had conducted a research to estimate the rate of soil formation for Ethiopia and found that the range of tolerable soil loss level for various agro-ecological zone of Ethiopia from 2 to 18 tons/ha. The simulated sediment yield in this study area was found to be in the tolerable rate as indicated in Table 11 and figure 13.

Table 11. Simulated sediment yield (t/ha) with respect to subbasin

	SUBBASIN								
Year	1	2	3	4	5	6	7	8	9
1994	0.544	0.199	1.052	1.552	0.733	2.129	0.514	1.493	0.644
1995	2.777	1.229	2.234	6.274	3.597	9.227	4.147	6.141	2.846
1996	8.061	3.619	17.961	43.612	10.172	64.423	11.563	43.421	21.296
1997	2.867	1.105	15.474	45.767	3.704	68.88	3.432	45.714	22.204
1998	4.296	2.233	1.79	6.134	5.627	8.945	4.947	5.707	2.711
1999	3.854	2.289	0.605	1.397	5.058	2.059	5.65	1.337	0.58
2000	5.873	2.438	0.58	2.105	7.385	3.152	7.417	2.066	0.935
2001	0.956	0.479	0.321	1.584	1.211	2.412	1.32	1.513	0.633
2002	1.349	0.596	0.167	0.792	1.741	1.213	1.699	0.758	0.329
2003	3.116	1.234	4.95	19.813	3.99	30.839	3.214	18.812	8.307
2004	0.378	0.186	0.01	0.103	0.483	0.161	0.704	0.099	0.037
2005	0.047	0.021	0	0	0.061	0	0.06	0	0
2006	7.528	3.656	0	0	9.746	0	7.285	0	0
2007	2.376	1.177	0.323	1.654	3.029	2.547	3.996	1.607	0.708
2008	4.71	1.961	0.561	2.524	6.046	3.874	6.474	2.482	1.072
Average	3.249	1.495	3.069	8.887	4.172	13.324	4.162	8.743	4.153

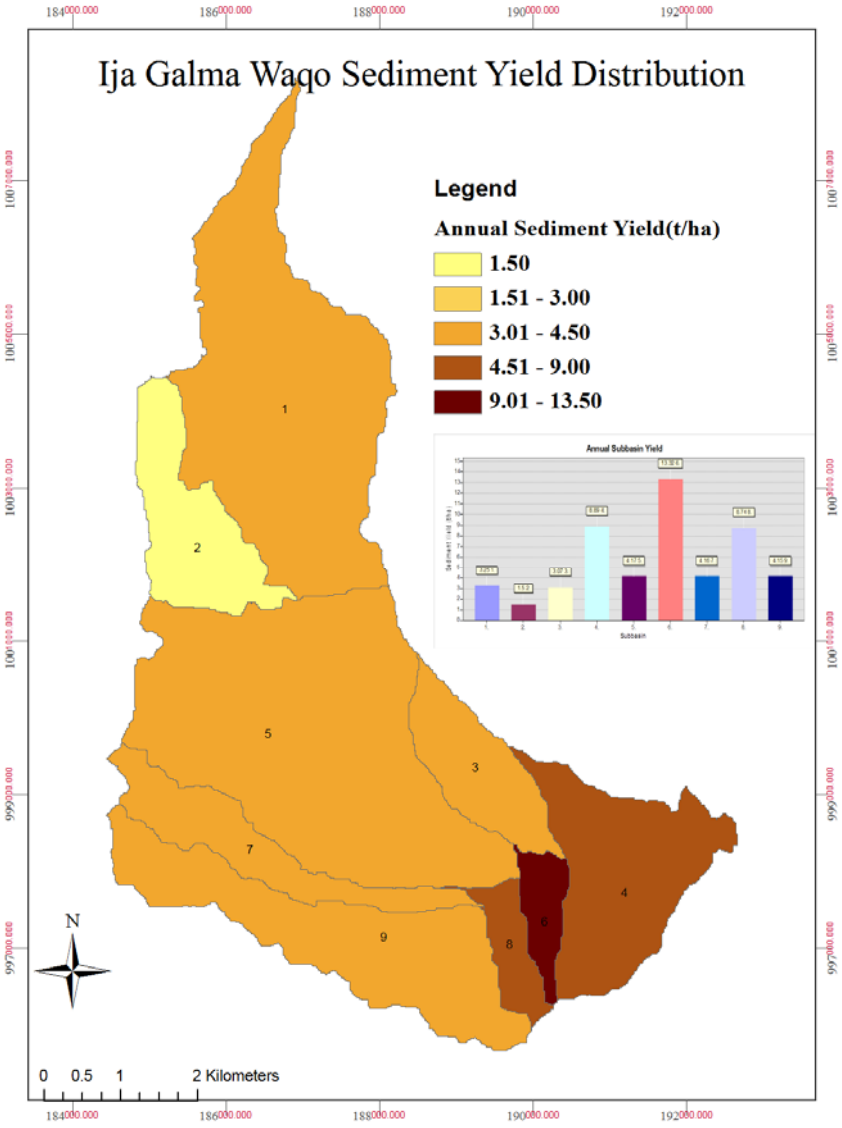

Figure 13. Sediment distribution with respect to subbasin

5. CONCLUSION AND RECOMMENDATION

5.1. Conclusion

Given the complexities of a watershed and the large number of interactive processes taking place simultaneously and consecutively at different times and places within a watershed, it is quite remarkable that the simulated results comply with the measurements to the degree that they do. Based on the results obtained in this study, SWAT is assessed to be a reasonable model to use for water quality (sedimentation) and water quantity studies in the Ija Galma Waqo watershed. On that positive note, however, a careful calibration and uncertainty analysis and proper application of modelling results should be exercised.

5.2. Recommendation

- Notwithstanding the data scarcity, the result is very satisfying and provides notable insight into the runoff availability and the associated uncertainties in this susceptible region.
- Subbasin no 6 of Ija Galma Waqo at the existing condition (agricultural land with $\geq$ 12.72% of which has a slope > 20%) generates a maximum annual average sediment yield of 13.3 ton/ha, this can be reduced by using sediment yield intervention strategies such as land slope stabilization, construction bench terraces, changing the land use of steepy area and afforestaion.
- As only river discharges were calibrated and validated, it has to be emphasized that other outputs presented in this study, such as sediment yield, have to be treated with caution. The model could be further tested when data on sediment load is available.
- Finally, Ija Galma Waqo spate irrigation project was designed with no adequate information and it was designed to supplement a minimum of 350 mm water but the study shows at 70% dependable flow the available water is 250 mm, this indicate that there is a high shortage of water. Therefore, this problem can be solved by reducing the hectare to be developed and by selecting appropriate crops which can be grown with minimum water and stress tolerant, with the availability of water.

6. REFERENCE

Allen, R. G., Pereira, L. S., Raes, D. I., Smith, M., 1998. Crop evaporation - Guidelines for computing crop water requirements, FAO Irrigation and drainage paper 56, http://www.fao.org/docrep/XO49OE/x0490e00.htm# Contents, Stand: 1 7. 10. 2002.

Arnold, J. G., 1993. A comprehensive surface-ground water flow model. J. Hydrol. 142:47-69.

Arnold, J. G., 1995. Automated base flow separation and recession analysis techniques. Groundwater 33(6): 1010-1018.

Arnold, J. G., 1999. Automated methods for estimating base flow and ground water recharge from stream flow records. J. of Amer. Water Res. Assoc. 35(2): 411-424.

Arnold, J. G., 2001. Hydrologic model for design of constructed wetlands. Wetlands 21(2):l67-178.

Arnold, J. G. and Allen. P. M., 1996. Estimating hydrologic budgets for three Illinois watersheds. J. Hydrol. 176:57-77.

Arnold, J. G. and Allen, P. M., 1999. Automated methods for estimating base flow and groundwater recharge from stream flow records. Water Resources Bulletin 35(2):411-424

Arnold, J. G., Srinivasan, R. and Engel, B. A., 1994. Flexible watershed configurations for simulation models. American Institute of Hydrology. Hydrol. Sci.Technol. 30(1-4): 5-14.

Arnold, J. G., Srinivasan, R., Muttiah, R. S. and Williams, J. R., 1998. Large area hydrologic modeling and assessment–Part 1: Model development. *Journal of the American Water Resources Association* **34**: 73–89.

Arnold, J. G., Muttiah. R. S., Srinivasan, R. and Allen, P. M. 2000. Regional estimation of base flow and groundwater recharge in the upper Mississippi basin. J. Hydrol. 227:2 1-40.

Bagnold, R. A., 1977. Bed load transport in natural rivers. Water Resour. Res. 13 (2), 303–312.

Benaman, J. and Shoemaker, C. A., 2004. Methodology for analyzing ranges of uncertain model parameters and their impact on total maximum daily load processes. J. Environ. Engr. 130(6): 648-656.

Benaman, J. and Shoemaker, C. A., 2005. An analysis of high-flow sediment event data for evaluating model performance. Hydrol. Process. 19(3): 605-620.

Bingner, R. L., 1996. Runoff Simulated from Goodwin Creek Watershed Using SWAT. Trans. ASAE39 (1): 85-90.

Bosch, J. M. and Hewlett, J. D., 1982. A review of catchment experiments to determine the effect of vegetation changes on water yield and evapotranspiration.

Bowling, L. C. and Lettenmaier, D. P., 1997. Evaluation of the effects of forest roads on stream flow in Hard and Ware creeks, Washington. University of Washington, Seattle, WA, USA Water Resources Series Technical Report, No. 155.

Brooks, K. N., Ffolliott, P. F., Gregersen, H. M. and Thames, J. L., 1991. Hydrology and the management of watersheds. Ames, Iowa: Iowa State University Press.

Bruijnzeel, L. A., 1990. Hydrology of moist tropical forests and effects of conversion: A state-of-knowledge review. Paris: UNESCO International Hydrological Programme.

Bruijnzeel, L. A. and Bremmer, C. N., 1989. Highland-lowland interactions in the Ganges-Brahniaputra river basin: A review of published literature. ICIMOD Occasional Paper, No. 11.

Calder, I.R., 1998. Water-resource and land use issues. SWIM Paper 3. Colombo: IIMI.

Chaplot, V., Saleh, A. Jaynes, D. B. and Arnold, J., 2004. Predicting water, sediment and No_3-N loads under scenarios of land-use and management practices in a flat watershed water air soil poliut. 154(1-4): 271-293.

Chomitz, K. M. and Kumari, K., 1996. The domestic benefits of tropical forests. A critical review emphasizing hydrologic functions. World Bank Policy Research Working Paper, No. 1601.44 Discussion paper I Land use impacts on water resources: a literature review

Chow, V.T., Maidment, D.R., Mays, L.W., 1988. Applied Hydrology. McGraw-Hill, New York.

Chu, T. W. and Shirmohammadi, A., 2004. Evaluation of the SWAT model's hyrodology component in the piedmont physiographic region of Maryland. Trans. ASAE 47(4):l057- 1073.

Conan, C., Marsily, G.de., Bouraoui, F. and Bidoglio, G., 2003. A long-term hydrological modelling of the Upper Guadiana river basin (Spain). Phys. Chem. Earth 28:193-200.

Deliberty, T. L. and Legates, D. R., 2003. Interannual and seasonal variability of modelled soil moisture in Oklahoma. lnt. J. CIin1atol. 23:1057-1086.

Ethiopian Highland Reclamation Study (EHRS), 1984. Annual Research Report (1983-l984) Ministry of Agriculture: Addis Ababa.

Eckhardt K. and J. G. Arnold, 2001. Automatic calibration of a distributed catchment model, Journal of Hydrology, vol. 251, no. 1/2, pp. 103-109.

Falkenmark, M. and Chapman, T. (eds)., 1989. Comparative Hydrology. An ecological approach to land and water resources, Paris: UNESCO.

Food and Agriculture Organization (FAO), 1987. Guidelines for economic appraisal of watershed management projects. in H. M. Gregersen, K. N. Brooks, J. A. Dixon and L. S. Hamilton. F'AO Conservation Guide No. 16. Rome, Italy.

Gitau, M., W., Veith, T. L. and Gburek, W. J., 2004. Farm-level optimization of BMP placement for cost effective pollution reduction. Trans. ASAE 47(6): 1923-1931.

Govender, M. and Everson. C. S., 2005. Modeling stream flow from two small South African experimental catchmcnts using the SWAT model. Hydrol. Process. 19(3): 683-692.

Green, W. H. and Ampt, G. A., 1911. Studies on soil physics, 1. The flow of air and water through soils. Journal of Agricultural Sciences 4:11-24.

Häckel, H., 1999. Meteorologie, Stuttgart: Ulmer, 4th edition.

Hargreaves, G. L., Hargreaves, G. H. and Riley, J. P., 1985. Agricultural benefits for Senegal River basin. J. Irrig. And Drain. Engr; 111(2): 113-124.

Hernandez, M., Miller, S. C.. Goodrich, D. C., Goff, B. F., Kepner, W. O., Edmonds, C. M. and Jones, K. B., 2000. Modeling runoff response to land cover and rainfall spatial variability in semi-arid watersheds. Environ. Monitoring Assess. 64:285-298.

Hofer, T., 1998. Do land use changes in the Himalayas affect downstream flooding?

Hooghoudt, S. B., 1940. Bijdrage tot de kennis van enige natuurkundige grootheden van de grond. Versl. Landbouwkd. Onderz. 46: 515-707.

Hurni, H., 1989. Soil for the Future. Environmental Research for Development Cooperation, Uni Press 62, University of Berne, Berne, pp. 42-46.

Ives, J. D. and Messerli, B., 1989. The Himalayan dilemma. Reconciling development and conservation. London: United Nations University Press.

Jayakrishnan, R., Srinivasan, R., Santhi, C. and Arnold, J. G., 2005. Advances in the application of the SWAT model for water resources management. Hydrol. Process. 19(3): 749-762.

Kaur, R., Singh, O., Srinivasan, R., Das, S. N. and Mishra, K., 2004. Comparison of a subjective and a physical approach for identification of priority areas for soil and water management in a watershed: a case study of Nagwan watershed in Hazaribagh District of Jharkhand, India. Environ. Model.Assess. 9(2): 115-127.

Kirsch, K., Kirsch, A. and Arnold, J. G., 2002. Predicting sediment and phosphorus loads in the Rock River Basin using SWAT. Trans. ASAIS 45(6):1757-1769.

Kroger et al., 1996. Creating and inventory of indigenous soil and water conservation measures n Ethiopia, in Scoons et al, Sustaining the Soil: Indigenous Soil and Water Conservation in Africa, Earth scan, London

La Marche, J. and Lettenmaier, D. P., 1998. Forest road effects on flood flows in the Deschutes river basin, Washington. University of Washington, Seattle. Water Resources Series Technical Report, No.1 58.

Mapfumo, E., Chanasyk, D. S. and Wilims, W.D., 2004. Simulating daily soil water under foothills fescuegrazing with the soil and water assessment tool model (Alberta, Canada). Hydrol. Process. 18:2787-2800.

Monteith, J. L., 1965. Evaporation and the Environment. *In:* The State and Movement of Water in Living Organisms. XIXth Symposium, Soc. for Exp. Biol., Swansea, Cambridge University Press, pp. 205-234.

Nash J. E., Sutcliff, J. V., 1970. River Flow Forcasting through Conceptual Models Part I- A discussion of Principles. Journal of Hydrology, 10:282-290.

Neitsch, S. I., Arnold, J. O., Kinrv, J. R. and Williams, J. R., 2005. Soil and Water Assessment Tool, Theoretical Documentation: Version 2005. Temple, TX. USDA Agricultural Research Service anti Texas A&5I Black land Research Center,

Peters, N. E. and Meybeck, M., 2000. Waler quality degradation effects on freshwater availability: Impacts of human activities. Water International, 25(2): 185-193.

Priestley, C. H. B., Taylor, R. J., 1972. On the assessment of surface heat flux and evaporation using large- scale parameters. Mon Weather. Rev. 100: 81-92.

Rosenthal, W. D. and Hoffman, D. W., 1999. Hydrologic modeling / GIS as an aid in locating monitoring sites. Trans. ASAE 42(6): 1591-1598.

Rosenthal, W. D., Srinivasan, R. and Arnold, J. G., 1995. Alternative river management using a linked GlS-hydrology model. Trans. ASAE 38(3):783-790.

Saleh, A., Arnold, J. G., Gassrnan, P. W., Hauck, L. W. Rosenthal, W. D., Williams, J. R. and McFarland, A.M.S., 2000. Application of SWAT for the Upper North Bosque Watershed. Trans. ASAE43 (5): 1077-1087.

Santhi, C., Arnold, J. G., Williams, J. R., Dugas, W. A., Srinivasan, R. and Hauck, L. M., 2001. Validation of the SWM model on a large river basin with point and nonpoint sources. J. of Amer. Water Res. Assoc. 37(5): 1l9-l 188. Page 1616

SCRP, 1996. Soil Conservation Research Project Database Report 1982—1993. Ministry of Agriculture and University of Berne, Series Report III. Hundelafto Research Unit, Institute of Geography, University of Berne, Switzerland.

Smedema, T. K. and Rycroft, D. W., 1983. Land drainage-planning and design of agricultural drainage systems, Cornell University Press, Ithica, N.Y.

Srinivasan, R. S., Arnold, J. G. and Jones, C. A., 1998. Hydrologic modeling of the United States with the soil and water assessment tool. Water Resour. Develop. 14(3): 315- 325.

Tejwani, K. G., 1993. Water management issues: Population Agriculture and Forests a focus on watershed management. In: Bonell, M., Hufschmidt, M. M. and Gladwell, J. S. Hydrology and water management in the humid tropics. Paris: UNESCO, pp 496-525.

Tripathi, M. P., Panda, R. K. and Raghuwanshi, N. S., 2003. Identification and Prioritization of Critical Sub-watersheds for Soil Conservation Management using the SWAT Model. Bio-systems Engineering (2003) 85(3):365-379, doi: 10.1016/SI 537- 5110(03)00066-7.

Tripathi, M. P., Panda, R. K. Raghuwanshi, N. S. and Singh, R., 2004. Hydrological modelling of a smallwatershed using generated rainfall in the soil and water assessment tool model. Hydrol. Process.18:181 l-1821.Page 1717

Tripathi, M. P., Panda, R. K. and Raghuwanshi, N. S., 2005. Development of effective management plan for critical watersheds using SWAT model. Hydrol. Process. 19(3): 809-826.

USDA Soil Conservation Service (SCS), 1972. National Engineering Handbook Section 4 Hydrology, Chapters 4-10,

Vaché, K. B., Eilers, J. M. and Santelman. M. V., 2002. Water quality modeling of alternative agricultural scenarios in the U. S. Corn Belt. J. of Amer. Water Res. Assoc. 38(2):773-787.

Van Liew, M. W. and Garbrecht, J., 2003. Hydrologic simulation of the Little Washita River experimental watershed using SWAT. J. of Amer. Water Res. Assoc. 39(2):413- 426.

van Griensven, A., 2005. Sensitivity, auto-calibration, uncertainty and model evaluation in SWAT2005.

van Griensven, A., Francos, A. and Bauwens, W., 2002. Sensitivity analysis and auto calibration of an integral dynamic model for river water quality. Water Sci. Technol. 45, 325-332.

van Griensven, A. and Green, C. H., 2007. Auto-calibration in Hydrological Modeling: Using SWAT2005in small-scale watersheds. Science Direct, Environmental Modeling & Software23 (2008), 422-434, available at: www.sciencedirect.com [Accessed 27 April 2009]

Williams, J. R., 1975. Sediment-yield prediction with universal equation using runoff energy factor p. 244-252. In Present and prospective technology for predicting sediment yield and sources: Proceedings of the sediment yield workshop, USDA Sedimentation Lab., Oxford, MS, November 28-30, 1972. ARS-S-40

Williams, J. R., 1980. SPNM, a model for predicting sediment, phosphorous, and nitrogen from agricultural basins. Water Resour. Bull. 16 (5), 843–848.

Williams, J. R., 1995. The EPIC model. P. 909-1000. In V.P. Singh (ed). Computer models of watershed hydrology. Water resources Publications, Highlands Ranch, CO.

Winchell, M.,. Srinivasan, R., Di Luzio, M., and Arnold, J., 2008. ArcSWAT 2.0 Interface for SWAT 2005, User Manual. 720 East Blackland Road- Temple, TEXAS 76502

Wischmeier, W.H. and Smith, D.D., 1978. Predicting rainfall erosion losses: a guide to conservation planning. Agriculture Handbook 282. USDA-ARS

Zemenfes T., 1995. The political economy of land degradation in Ethiopia. Northeast African Studies;2:7198.

7. APPENDICES

7.1. Appendix I. Meteorological and Hydrological Data Tables

Appendix Table 1. Statistical precipitation data (1981 - 2000) and temperature for Haramaya station

Item	Month											
	Jan.	Feb.	Mar.	Apr.	May.	Jun.	Jul.	Aug.	Sep.	Oct.	Nov.	Dec.
PCP_MM	8.18	22.59	62.89	112.58	112.96	46.88	103.30	132.85	114.04	45.72	17.32	6.30
PCPSTD	21.14	23.37	65.03	48.16	60.22	30.53	53.24	60.31	43.51	51.21	22.79	11.45
PCPSKW	8.72	6.91	6.21	3.53	3.95	5.07	4.05	3.07	3.17	5.00	9.63	10.80
PR_W1	0.03	0.09	0.19	0.30	0.29	0.25	0.40	0.46	0.42	0.11	0.06	0.04
PR_W2	0.86	0.72	0.67	0.70	0.67	0.64	0.63	0.67	0.71	0.74	0.81	0.88
PCPD	7.92	7.16	11.72	15.92	15.08	12.80	16.68	18.68	18.64	10.16	8.20	9.68
TMPMX	23.00	24.57	25.48	25.42	25.58	24.92	23.92	23.42	23.61	23.76	23.30	22.37
TMPSTDMX	1.89	1.92	1.85	2.05	1.75	1.85	2.06	1.71	1.17	1.43	1.45	1.40
TMPMN	6.84	6.77	10.77	12.40	13.57	13.96	13.47	13.49	12.72	8.32	4.84	4.82
TMPSTDMN	4.49	4.38	3.58	2.71	2.06	0.99	0.65	0.72	1.76	3.84	3.93	4.17
WNDAV	1.80	2.01	2.13	1.94	2.02	2.83	2.78	2.24	1.40	1.14	1.39	1.55
RH(%)	73.09	75.60	79.75	77.18	83.18	84.78	85.50	84.78	85.00	83.29	80.40	76.00
SOLARAV	18.40	19.70	20.20	18.90	18.20	16.30	15.30	15.40	18.10	20.20	19.60	19.20
TDEW	11.29	11.73	11.79	13.07	13.51	13.98	13.85	14.62	13.86	12.00	10.22	9.02

Where:

PCP_MM : average monthly precipitation (mm)
PCPSTD : standard deviation
PCPSKW : skew coefficient
PR_W1 : probability of a wet day following a dry day
PR_W2 : probability of a wet day following a wet day
PCPD : average number of days of precipitation in month
TMPMX: Average or mean daily maximum air temperature for month ºC).
TMPSTDMX : Standard deviation for daily maximum air temperature in month (ºC).
TMPMN: Average or mean daily minimum air temperature for month (ºC).
TMPSTDMN: Standard deviation for daily minimum air temperature in month (ºC).
SOLARAV (mon): Average daily solar radiation for month (MJ/m2/day).
DEWPT (mon): Average daily dew point temperature in month (ºC).
WNDAV (mon): Average daily wind speed in month (m/s).

Appendix Table 2. Haramaya total monthly precipitation (mm)

	Month												
Year	Jan.	Feb.	Mar.	Apr.	May.	Jun.	Jul.	Aug.	Sep.	Oct.	Nov.	Dec.	Total
1981	4.2	8.4	239.3	168.3	120.2	16.2	122.7	204.7	142.0	15.2	2.6	0.0	1043.80
1982	3.1	57.8	61.6	92.0	141.7	31.2	85.4	122.1	87.6	158.8	38.1	11.0	890.40
1983	0.0	25.7	13.3	80.9	176.3	75.3	116.1	300.6	151.4	23.5	4.2	0.0	967.30
1984	0.0	0.0	0.0	25.6	167.7	71.9	**67.6**	101.6	100.2	0.0	17.5	6.7	558.84
1985	0.0	0.0	46.9	**128.0**	87.6	29.7	88.3	80.2	69.6	9.9	6.1	0.0	546.34
1986	0.0	38.6	14.1	153.9	110.1	80.8	66.1	161.4	96.7	34.0	5.8	0.0	761.50
1987	0.0	8.1	180.2	148.6	248.2	29.6	63.3	123.2	111.9	28.8	2.7	0.0	944.60
1988	9.8	43.8	30.4	154.3	31.3	54.1	101.5	173.7	173.4	41.9	0.0	6.0	820.20
1989	0.0	14.4	154.9	114.5	69.4	52.6	104.0	146.0	104.4	41.2	3.6	45.0	850.00
1990	1.7	73.1	45.4	132.3	59.6	54.1	80.9	162.3	133.8	53.3	0.0	7.0	803.50
1991	0.0	51.7	36.2	73.2	58.6	25.7	108.3	104.8	120.1	25.8	**0.0**	**0.0**	604.40
1992	3.9	11.0	18.2	85.2	65.1	68.3	77.5	97.6	107.1	36.6	10.4	4.1	585.00
1993	**46.2**	**38.9**	**3.0**	**206.8**	**105.9**	**31.0**	**59.3**	**92.7**	**102.4**	**109.1**	**0.0**	**0.0**	795.31
1994	**0.0**	**0.0**	**28.3**	**91.4**	**157.6**	**15.9**	**261.6**	**139.9**	**181.3**	**5.2**	**74.4**	**0.0**	955.54
1995	**0.0**	**23.7**	**108.5**	**195.6**	**93.1**	**44.9**	**128.0**	**109.3**	**87.3**	**9.6**	**0.0**	**9.1**	809.06
1996	**8.3**	**2.0**	**104.6**	**76.9**	**226.2**	**136.8**	**184.0**	**201.3**	**153.7**	**0.9**	**24.2**	**0.0**	1118.96
1997	0.0	0.0	78.1	125.4	155.9	59.8	148.7	102.7	61.7	194.1	60.4	**6.0**	992.77
1998	86.5	51.0	20.3	59.9	55.4	24.8	116.5	104.4	175.7	54.0	21.3	0.0	769.80
1999	0.0	3.7	68.3	77.5	77.4	0.0	0.0	0.0	0.0	37.2	17.1	1.6	282.80
2000	**0.0**	**0.0**	**6.3**	**61.3**	**51.9**	**35.0**	**86.1**	**128.4**	**120.5**	**35.3**	**58.0**	**29.5**	612.25
Mean	8.18	22.59	62.89	112.58	112.96	46.88	103.30	132.85	114	45.72	17.32	6.30	785.62
Stdv	21.14	23.37	65.03	48.16	60.22	30.53	53.24	60.31	43.51	51.21	22.79	11.45	203.99

Source: MoWR. (Bold values are Estimate)

Appendix Table 3. Statistical precipitation data (1995 - 2005) for Harar rainfall and temperature

	Month											
Item	Jan.	Feb.	Mar.	Apr.	May.	Jun.	Jul.	Aug.	Sep.	Oct.	Nov.	Dec.
PCP_MM	14.49	10.78	74.96	105.39	78.53	88.61	128.86	164.52	126.03	44.15	16.96	14.00
PCPSTD	25.05	13.12	44.02	91.19	51.23	38.43	62.70	93.32	78.67	54.69	23.92	16.97
PCPSKW	9.46	5.83	4.36	4.51	3.33	4.91	3.45	3.99	6.53	5.21	6.79	7.58
PR_W1	0.03	0.04	0.16	0.27	0.25	0.26	0.33	0.34	0.32	0.13	0.05	0.03
PR_W2	0.89	0.90	0.73	0.73	0.71	0.76	0.69	0.78	0.75	0.84	0.88	0.93
PCPD	10.00	10.57	12.00	15.71	15.50	17.00	16.36	20.14	17.79	15.14	10.50	11.79
TMPMX	26.82	28.09	28.12	27.39	26.66	25.74	24.51	24.92	25.79	26.43	26.49	26.35
TMPSTDMX	2.27	1.99	2.32	2.32	1.37	2.11	2.26	1.70	1.57	2.32	1.71	1.34
TMPMN	11.71	12.42	13.44	13.77	13.89	13.81	13.56	13.66	13.15	13.02	11.96	11.30
TMPSTDMN	1.86	1.83	1.43	1.19	1.17	1.04	0.99	1.12	0.92	1.41	1.80	1.82
WNDAV	1.51	1.26	1.21	0.95	0.83	0.81	0.74	0.73	0.69	0.71	0.97	1.29
RH	70.60	71.20	79.20	85.40	88.00	89.00	87.33	85.50	87.17	82.20	75.75	70.00
SOLARAV	20.00	19.80	20.40	20.40	19.90	18.80	18.10	17.90	18.70	19.90	19.60	19.10
TDEW	15.19	16.36	18.37	19.19	19.23	18.79	17.62	17.58	18.27	17.71	16.14	14.63

Appendix Table 4. Harar total monthly precipitation (mm)

	Month												
Year	Jan.	Feb.	Mar.	Apr.	May.	Jun.	Jul.	Aug.	Sep.	Oct.	Nov.	Dec.	Total
1995	0.0	24.6	112.2	318.1	67.1	55.3	114.6	108.4	38.9	3.4	0.0	25.3	*867.9*
1996	9.2	2.4	83.1	33.8	171.5	131.0	114.1	175.2	181.0	0.0	9.6	0.0	*910.9*
1997	0.0	0.0	**72.1**	**159.0**	150.5	**137.4**	54.4	67.4	12.0	136.8	17.2	20.6	*827.3*
1998	59.0	38.4	16.5	4.3	59.5	47.5	59.0	32.9	**229.6**	29.7	20.5	0.0	*596.9*
1999	0.0	3.0	80.7	77.4	55.3	123.8	117.2	141.7	58.1	154.2	0.0	0.0	*811.4*
2000	0.0	0.0	2.0	114.4	79.9	24.0	72.2	98.8	78.3	12.3	79.9	54.3	*616.1*
2001	0	5	54.5	39	99	63.4	114.9	357.8	170.9	8.9	0	11.5	*924.9*
2002	69.1	8.2	85.5	74.8	29	129.2	122.5	208.9	112.6	31.7	0		*871.5*
2003	10.6	26.5	61.7	74	22.6	84	219.4	258.8	219	31	5	15.7	*1028.3*
2004	11.5	0	90.9	206.6	14.7	83.7	183.1	137.8	210.9	76	17.5	12.6	*1045.3*
2005	0	10.5	165.4	57.9	114.7	95.4	246.1	222	75	1.7	36.9	0	*1025.6*
Mean	14.49	10.78	74.96	105.39	78.53	88.61	128.86	164.52	126.03	44.15	16.96	14.00	866.02
Stdv	25.05	13.12	44.02	91.19	51.23	38.43	62.70	93.32	78.67	54.69	23.92	16.97	151.26

Source: MoWR. (Bold values are Estimate)

Appendix Table 5. Hydrological data for Erer gauging station (m^3/s)

	Month												
Year	Jan	Feb	Mar	Apr	May	Jun	Jul	Aug	Sep	Oct	Nov	Dec	Average(m^3/s)
1984	0.19	0.12	0.08	0.07	0.80	0.51	0.43	0.90	0.78	0.58	0.04	0.00	0.37
1985	0.00	0.00	0.00	0.61	0.84	0.91	0.40	1.11	0.79	0.29	0.00	0.00	0.41
1986	0.00	0.00	0.00	0.00	0.44	0.72	0.98	0.38	0.65	0.73	0.21	0.14	0.35
1987	0.06	0.07	0.19	2.26	4.34	0.51	0.21	0.31	1.33	0.18	0.06	0.00	0.79
1988	0.00	0.00	0.00	1.52	0.05	0.18	0.31	6.79	10.71	6.59	1.29	0.00	2.29
1989	0.00	0.00	0.56	5.45	1.93	1.14	1.99	2.87	3.96	1.04	0.37	0.07	1.62
1990	0.00	0.00	0.00	0.81	0.45	0.00	0.23	3.04	3.38	1.04	0.00	0.16	0.76
1991	0.53	0.53	0.53	1.27	1.43	0.88	1.65	1.43	0.73	0.21	0.19	0.14	0.79
Mean	0.10	0.09	0.17	1.50	1.28	0.61	0.78	2.10	2.79	1.33	0.27	0.06	0.92
STDEV	0.19	0.18	0.24	1.77	1.37	0.38	0.69	2.15	3.45	2.15	0.43	0.07	0.68

Source: MoWR.

Appendix Table 6. Simulation result of average daily flow (m^3/s) in month for the Erer guaging station

	Month												
Year	Jan	Feb	Mar	Apr	May	Jun	Jul	Aug	Sep	Oct	Nov	Dec	Average
1984	0.608	0.074	0.006	0.025	0.886	1.130	0.345	0.536	1.564	0.040	0.013	0.006	0.435
1985	0.000	0.001	0.191	1.602	0.172	0.039	0.245	0.590	0.363	0.025	0.007	0.014	0.271
1986	0.001	0.004	0.004	1.351	1.189	0.207	0.236	1.417	1.267	0.541	0.067	0.023	0.528
1987	0.015	0.001	0.347	2.375	5.606	0.229	0.785	0.463	2.142	0.908	0.046	0.034	1.087
1988	0.068	0.017	0.037	3.228	0.793	0.015	0.044	6.734	4.562	2.098	0.031	0.011	1.472
1989	0.005	0.005	0.726	3.208	0.545	0.041	0.311	1.688	1.726	0.131	0.066	0.565	0.752
1990	0.007	0.107	0.159	1.324	0.519	0.672	0.045	1.000	3.790	1.676	0.043	0.015	0.778
1991	0.009	0.612	0.155	0.240	0.132	0.029	0.816	0.397	1.856	0.239	0.019	0.942	0.449

7.2. Appendix II. Homogeneity Test Result

Homogeneity test annual rainfall for Harar station result

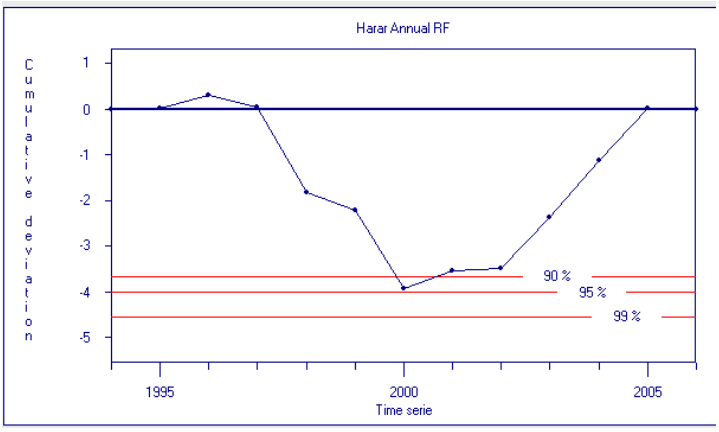

This graph was used to determine the position of change points. At points where the cumulative deviation sum plot shows a clear change of slope, it is assumed that there is a change in trend estimates of change point (year) is 2000

Appendix Figure 1. Rescaled cumulative deviation of annual rainfall Harar station

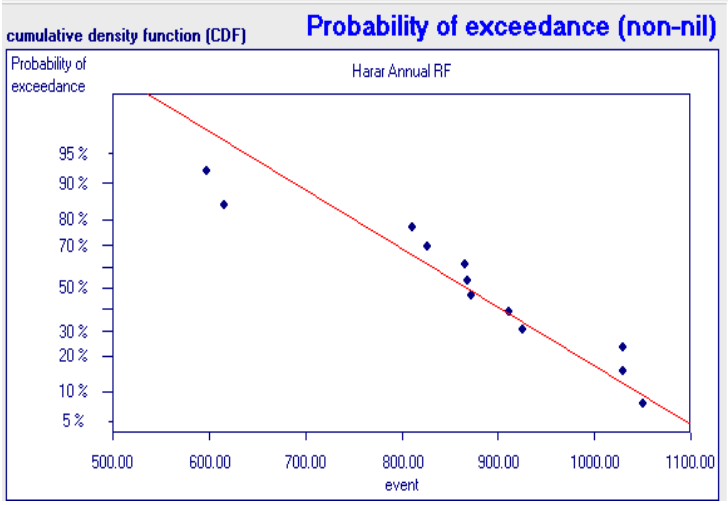

The probability plot of annual rainfall is given Appendix Figure A.4. The least square fit R^2 is 0.91

Appendix Figure 2. Probability plot of annual rainfall Harar station

Appendix Table 7. Probability of rejecting homogeneity of annual rainfall (Harar station)

	Rejected?		
Statistics	90%	95%	99%
Range of Cumulative deviation	No	No	No
Maximum Cumulative deviation	Yes	No	No

Closeness of linear relationship (CDF) R^2 =0.91

Homogeneity test for average annual flow for Erer gauging station

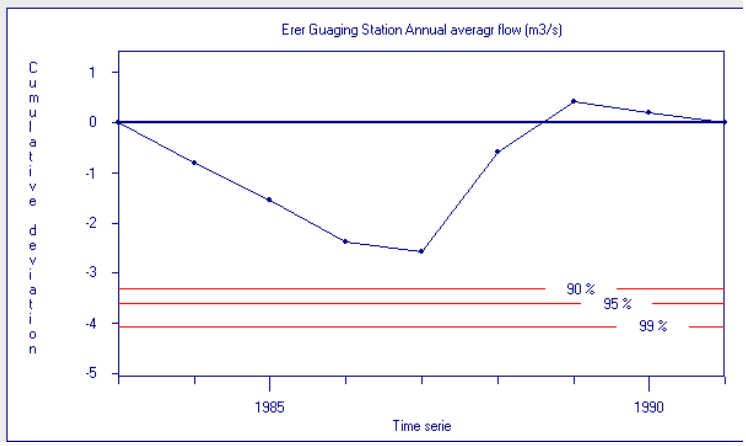

This graph was used to determine the position of change points. At points where the cumulative deviation sum plot shows a clear change of slope, it is assumed that there is a change in trend estimates of change point (year) is 1987

Appendix Figure 3. Rescaled cumulative deviation of annual mean flow Erer gauging station

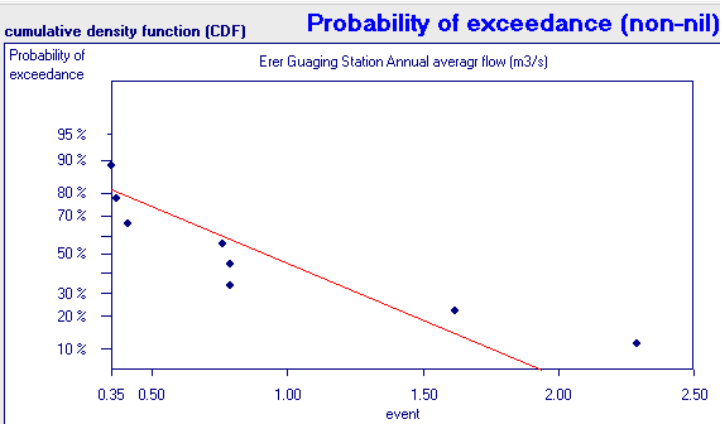

The probability plot of annual average flow is given Appendix Figure A.6. The least square fit R^2 is 0.81

Appendix Figure 4. Probability plot of annual average flow (m^3/s) Erer gauging station

Appendix Table 8. Probability of rejecting homogeneity of annual average flow (Erer station)

	Rejected?		
Statistics	90%	95%	99%
Range of Cumulative deviation	No	No	No
Maximum Cumulative deviation	No	No	No

Closeness of linear relationship (CDF) R^2 =0.81 Poor

7.3. Appendix III. Soil Data Parameter Value for each Soil Type

Appendix Table 9. Soil parameter value for Chromic Luvisols

Soil Hydrologic Group: D

Maximum rooting depth (mm): 1800.00

Porosity fraction from which anions are excluded: 0.500

Crack volume potential of soil: 0.500

Texture: Clay

Layer	1	2	3	4
Depth [mm]:	300	700	1100	1800
Bulk Density [g/cc]:	1.31	1.35	1.4	1.3
Ave. AW (Incl. Rock) Fraction	0.11	0.12	0.19	0.12
Ksat. [mm/hr]	0.28	0.35	23.66	0.83
Organic Carbon [weight %]	0.4	0.2	0.2	0.1
Clay [weight %]	59	54	18	55
Silt [weight %]	15	15	55	23
Sand [weight %]	26	31	27	22
Rock Fragments [vol. %]	0	0	0	0
Soil Albedo (Moist)	0.25	0.25	0.25	0.25
Erosion K	0.12	0.13	0.2	0.14
Salinity (EC)	0.3	0.8	0.3	0.2

Source: MoWR and computation

Appendix Table 10. Soil parameter value for Calcic Vertisols

Soil Hydrologic Group: D

Maximum rooting depth (mm): 2000.00

Porosity fraction from which anions are excluded: 0.500

Crack volume potential of soil: 0.500

Texture: C

Layer	1	2	3	4
Depth [mm]:	160	800	1300	2000
Bulk Density [g/cc]:	1.21	1.19	1.17	1.18
Ave. AW (Incl. Rock) Fraction	0.12	0.1	0.11	0.11
Ksat. [mm/hr]	4.76	3.15	2.35	1.99
Organic Carbon [weight %]	2.4	2.1	0.9	0.6
Clay [weight %]	50	69	79	77
Silt [weight %]	41	25	17	18
Sand [weight %]	9	6	4	5
Rock Fragments [vol. %]	0	0	0	0
Soil Albedo (Moist)	0.09	0.11	0.25	0.25
Erosion K	0.16	0.15	0.19	0.18
Salinity (EC)	0.1	0.2	0.3	0.9

Source: MoWR and computation

Appendix Table 11. Soil parameter value for Eutric Cambisols

Soil Hydrologic Group: D

Maximum rooting depth (mm): 1800.00

Porosity fraction from which anions are excluded: 0.500

Crack volume potential of soil: 0.100

Texture: SC

Layer	1	2	3	4
Depth [mm]:	300	800	1200	1800
Bulk Density [g/cc]:	1.38	1.48	1.49	1.29
Ave. AW (Incl. Rock) Fraction	0.11	0.12	0.11	0.11
Ksat. [mm/hr]	1.33	1.88	1.69	0.88
Organic Carbon [weight %]	1.5	0.9	0.8	1.5
Clay [weight %]	45	46	38	55
Silt [weight %]	22	18	16	24
Sand [weight %]	33	36	46	21
Rock Fragments [vol. %]	0	0	0	0
Soil Albedo (Moist)	0.16	0.25	0.25	0.16
Erosion K	0.12	0.13	0.14	0.12
Salinity (EC)	0.2	0.7	1.9	

Source: MoWR and computation

Appendix Table 12. Soil parameter value for Rendzic Leptosols

Soil Hydrologic Group: D

Maximum rooting depth (mm): 300.00

Porosity fraction from which anions are excluded: 0.500

Crack volume potential of soil: 0.100

Texture C

Layer	1
Depth [mm]:	300
Bulk Density [g/cc]:	1.19
Ave. AW (Incl. Rock) Fraction	0.11
Ksat. [mm/hr]	6.09
Organic Carbon [weight %]	3.5
Clay [weight %]	51
Silt [weight %]	38
Sand [weight %]	11
Rock Fragments [vol. %]	0
Soil Albedo (Moist)	0.04
Erosion K	0.15
Salinity (EC)	0.109

Source: MoWR and computation

Appendix Table 13. Soil parameter value for Haplic Phaezems

Soil Hydrologic Group: D

Maximum rooting depth (mm): 2000.00

Porosity fraction from which anions are excluded: 0.500

Crack volume potential of soil: 0.500

Texture C

Layer	1	2	3	4
Depth [mm]:	300	600	1500	2000
Bulk Density [g/cc]:	1.31	1.26	1.29	1.23
Ave. AW (Incl. Rock) Fraction	0.12	0.1	0.12	0.12
Ksat. [mm/hr]	0.93	1.1	0.74	0.78
Organic Carbon [weight %]	1.6	2	0.7	0.5
Clay [weight %]	53	59	55	61
Silt [weight %]	23	24	25	24
Sand [weight %]	24	17	20	15
Rock Fragments [vol. %]	0	0	0	0
Soil Albedo (Moist)	0.15	0.12	0.25	0.25
Erosion K	0.11	0.11	0.14	0.15
Salinity (EC)	0.1	0.1	0.1	0.1

Source: MoWR and computation

Appendix Table 14. Soil parameter value for Vertic Luvisols

Soil Hydrologic Group: D

Maximum rooting depth (mm): 2000.00

Porosity fraction from which anions are excluded: 0.500

Crack volume potential of soil: 0.500

Texture: C

Layer	1	2	3
Depth [mm]:	300	900	2000
Bulk Density [g/cc]:	1.3	1.24	1.28
Ave. AW (Incl. Rock) Fraction	0.12	0.11	0.12
Ksat. [mm/hr]	0.77	0.75	0.56
Organic Carbon [weight %]	1.2	0.7	0.4
Clay [weight %]	50	66	57
Silt [weight %]	21	18	23
Sand [weight %]	29	16	20
Rock Fragments [vol. %]	0	0	0
Soil Albedo (Moist)	0.2	0.25	0.25
Erosion K	0.12	0.13	0.14
Salinity (EC)	0.3	1.1	2.4

Source: MoWR and computation

Appendix Table 15. Soil parameter value for Humic Nitisol

Soil Hydrologic Group: D

Maximum rooting depth (mm): 2000.00

Porosity fraction from which anions are excluded: 0.500

Crack volume potential of soil: 0.500

Texture: C

Layer	1	2	3
Depth [mm]:	200	700	2000
Bulk Density [g/cc]:	1.23	1.13	1.23
Ave. AW (Incl. Rock) Fraction	0.11	0.063	0.13
Ksat. [mm/hr]	1.32	0.9	3.07
Organic Carbon [weight %]	2.4	1.4	0.6
Clay [weight %]	61	77	55
Silt [weight %]	26	15	36
Sand [weight %]	13	8	9
Rock Fragments [vol. %]	0	0	0
Soil Albedo (Moist)	0.09	0.17	0.25
Erosion K	0.12	0.12	0.2
Salinity (EC)	0.1	0.2	0.2

Source: MoWR and computation

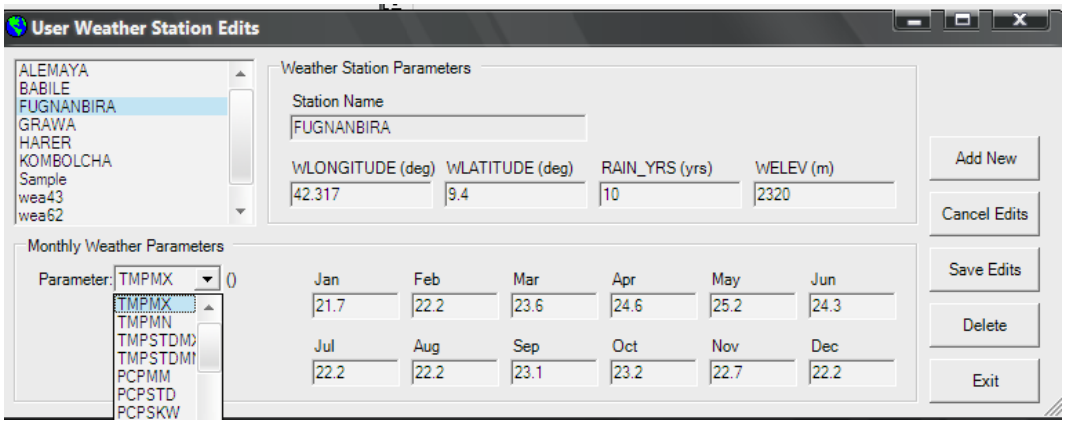

Appendix Figure 5. Weather station entry menu

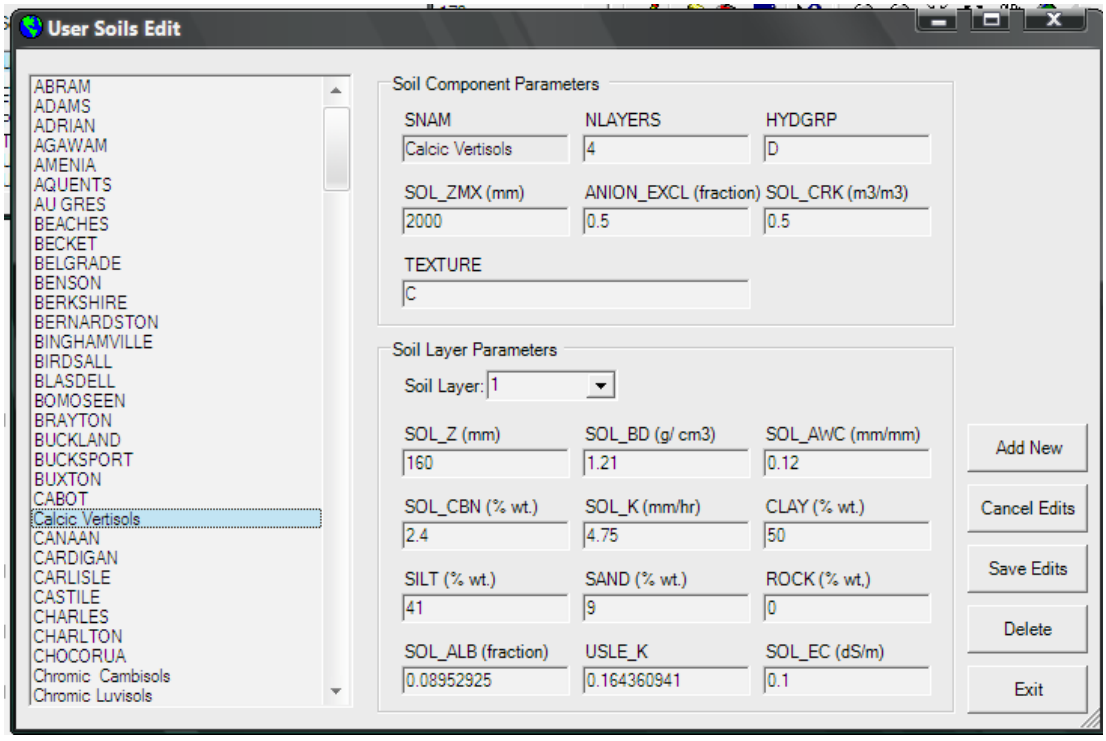

Appendix Figure 6. Soil data entry menu

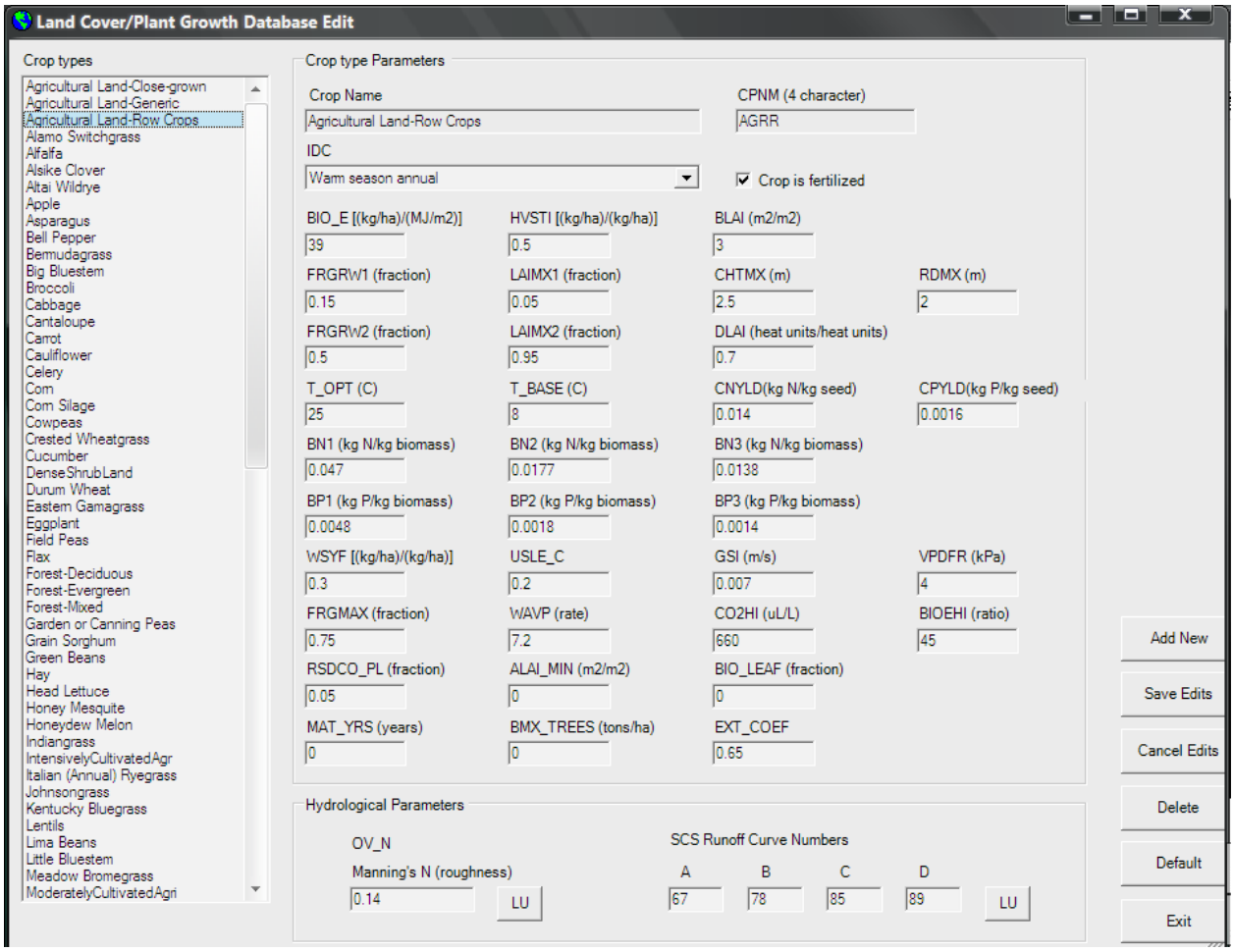

Appendix Figure 7. Land cover plant growth entry menu